

Article

# Dopamine Receptor Ligand Selectivity—An In Silico/In Vitro Insight

Lukas Zell, Alina Bretl, Veronika Temml  and Daniela Schuster \* 

Department of Pharmaceutical and Medicinal Chemistry, Institute of Pharmacy, Paracelsus Medical University, 5020 Salzburg, Austria; lukas.zell@pmu.ac.at (L.Z.); alina.bretl@pmu.ac.at (A.B.); veronika.temml@pmu.ac.at (V.T.)

\* Correspondence: daniela.schuster@pmu.ac.at; Tel.: +43-699-14420025

**Abstract:** Different dopamine receptor (DR) subtypes are involved in pathophysiological conditions such as Parkinson's Disease (PD), schizophrenia and depression. While many DR-targeting drugs have been approved by the U.S. Food and Drug Administration (FDA), only a very small number are truly selective for one of the DR subtypes. Additionally, most of them show promiscuous activity at related G-protein coupled receptors, thus suffering from diverse side-effect profiles. Multiple studies have shown that combined in silico/in vitro approaches are a valuable contribution to drug discovery processes. They can also be applied to divulge the mechanisms behind ligand selectivity. In this study, novel DR ligands were investigated in vitro to assess binding affinities at different DR subtypes. Thus, nine D<sub>2</sub>R/D<sub>3</sub>R-selective ligands (micro- to nanomolar binding affinities, D<sub>3</sub>R-selective profile) were successfully identified. The most promising ligand exerted nanomolar D<sub>3</sub>R activity (K<sub>i</sub> = 2.3 nM) with 263.7-fold D<sub>2</sub>R/D<sub>3</sub>R selectivity. Subsequently, ligand selectivity was rationalized in silico based on ligand interaction with a secondary binding pocket, supporting the selectivity data determined in vitro. The developed workflow and identified ligands could aid in the further understanding of the structural motifs responsible for DR subtype selectivity, thus benefitting drug development in D<sub>2</sub>R/D<sub>3</sub>R-associated pathologies such as PD.

**Keywords:** dopamine receptor; subtype selectivity; GPCR; in silico; molecular docking; secondary binding pocket; in vitro; HTRF



**Citation:** Zell, L.; Bretl, A.; Temml, V.; Schuster, D. Dopamine Receptor Ligand Selectivity—An In Silico/In Vitro Insight. *Biomedicines* **2023**, *11*, 1468. <https://doi.org/10.3390/biomedicines11051468>

Academic Editor: Floriana Volpicelli

Received: 14 April 2023

Revised: 3 May 2023

Accepted: 9 May 2023

Published: 17 May 2023



**Copyright:** © 2023 by the authors. Licensee MDPI, Basel, Switzerland. This article is an open access article distributed under the terms and conditions of the Creative Commons Attribution (CC BY) license (<https://creativecommons.org/licenses/by/4.0/>).

## 1. Introduction

G-protein coupled receptors (GPCRs) are one of the most prominent protein families targeted in drug research. Currently, they are represented by 475 approved (by the FDA) drugs acting on 108 different GPCRs [1]. Sixty-five of them target an essential sub-group of GPCRs, the dopamine receptor (DR) family, consisting of the subtypes 1, 2, 3, 4 and 5 (D<sub>1</sub>R, D<sub>2</sub>R, D<sub>3</sub>R, D<sub>4</sub>R and D<sub>5</sub>R, respectively) [2]. The DR family is divided into D<sub>1</sub>like-(D<sub>1</sub>R and D<sub>5</sub>R) and D<sub>2</sub>like receptors (D<sub>2</sub>R, D<sub>3</sub>R and D<sub>4</sub>R) and plays a crucial role in physiological processes such as a motoric function, cognition, sleep and memory [3]. However, it is also involved in many devastating diseases of the central nervous system (CNS) such as Parkinson's Disease (PD), schizophrenia and bipolar disorders. DR-targeting drugs act in different ways acting as, e.g., agonists in PD by activating the receptor, antagonists in schizophrenia by blocking the receptor or partial agonists used in treating bipolar disorders or addiction [3–5].

While all of the listed diseases are connected to the dopaminergic system, they are also characterized by a distinct dysfunctionality of different dopaminergic projection pathways [6]. In PD, the degeneration of dopaminergic neurons in the substantia nigra leads to reduced dopamine levels, thus reducing activation of the D<sub>2</sub>R [4]. In contrast, schizophrenia is defined by hyperproductive, presynaptical dopaminergic neurons in the mesolimbic region, thus overactivating the D<sub>2</sub>R. At the same time, dopaminergic neurons

in the prefrontal cortex are hypofunctional, resulting in insufficient activation of the D<sub>1</sub>R due to a lack of dopamine [3]. On the one hand, aberrant signalling involving the D<sub>3</sub>R has been implicated in diseases such as PD, restless leg syndrome and depression, where agonists are used to treat motor dysbalances. On the other hand, D<sub>3</sub>R antagonists have been shown to be useful as antipsychotics [7,8].

For most of those conditions, DR-targeting drugs have been approved by the FDA, successfully ameliorating major symptoms [2]. At the same time, they suffer from major drawbacks due to promiscuous activity at the DR subtypes other than the intended one, as well as closely related GPCRs [9]. Levodopa (L-DOPA), the gold standard in treating PD, successfully reduces the major motoric symptoms, such as bradykinesia and tremor, after biotransformation to dopamine, subsequently activating the D<sub>2</sub>R. Problematically, L-DOPA (and dopamine, respectively) is also known to induce dyskinesia (L-DOPA-induced dyskinesia) due to the promiscuous activation of the D<sub>1</sub>R in long-term treatment conditions [10]. While D<sub>2</sub>R agonists play an important role in treating PD, antagonists act as potent antipsychotics in different psychiatric disorders associated with the DR family. Those antipsychotics are also tightly connected to serious adverse drug events such as extrapyramidal syndrome and neuroleptic malignant syndrome [11,12].

D<sub>2</sub>R-selective drugs are clearly beneficial in treating PD and psychiatric disorders by alleviating the mentioned off-target effects. However, DR-subtype selectivity should not only be seen as a tool to counteract side effects but also to open up novel therapeutic avenues. Selective D<sub>3</sub>R agonists have been shown to be effective in vivo by mitigating the cell death of dopaminergic neurons and improving behavioural performances in mouse models of PD [13,14]. Interesting results have also been obtained in clinical studies establishing pramipexole (a D<sub>3</sub>R-preferring ligand) as an effective dopamine substitute in patients not responding to L-DOPA treatment, simultaneously delaying dyskinesia [15]. Another in vivo study indicated the capability of D<sub>3</sub>R-preferring agonists to reverse motivational deficits related to PD [16]. D<sub>3</sub>R-selective antagonists present a promising opportunity in the treatment of schizophrenia. They appear to be completely devoid of the D<sub>2</sub>R-associated side effects described earlier and also treat negative symptoms, which are not covered by conventional antipsychotics [17,18]. Selective D<sub>1</sub>R agonists are particularly interesting in treating cognitive deficits affecting patients suffering from schizophrenia by targeting the prefrontal cortex. Since the clinical relevance of D<sub>1</sub>R agonists was recognized early on, several selective compounds with diverse chemical scaffolds have been designed throughout the years [19]. While many selective ligands are considered a success, they also suffer from limited oral bioavailability and poor blood–brain barrier (BBB) permeability, thus exposing them to rapid peripheral metabolism. This has mainly been attributed to the presence of catechol functionalities in many of the ligands [20]. Different agonists have shown promising results in improving cognitive impairments and working memory in schizophrenia [21–23]. Unfortunately, other studies have provided evidence for D<sub>1</sub>R agonists being responsible for inducing seizures [24,25]. While the seizure-inducing mechanisms and the involvement of structure–activity relationships (SAR) are still not fully understood, the development of novel, potentially non-catechol agonists continues [19,26]. All of these findings clearly indicate the benefits of DR-subtype selective drugs. Moreover, they highlight the necessity of better understanding the molecular mechanisms involved in DR–ligand interactions to rationalize the SARs responsible for specific effects.

Drug research in the field of GPCRs has been benefitting from the ‘golden age of GPCR structural biology’ in the discipline of cheminformatics [27]. Different studies have been utilizing computer-assisted drug-design (CADD) methods to investigate GPCRs and also different DR subtypes [28–30]. A particularly interesting study by Bueschbell et al. investigated the selectivity of several known DR ligands (e.g., apomorphine and bromocriptine) with homology modelling and molecular docking approaches [31]. The ever-increasing availability of X-ray or cryo-EM structures of the discussed DR subtypes, D<sub>1</sub>R, D<sub>2</sub>R and D<sub>3</sub>R, aids our ability to comprehend DR ligand selectivity. In total, twelve three-dimensional (3D) protein structures of the D<sub>1</sub>R, five D<sub>2</sub>R structures and three D<sub>3</sub>R

structures are accessible in the Protein Data Bank (PDB) database as of March 2023. The advent of cryo-EM technologies enabled the high-resolution depiction of the complex DR subtype structures at  $\leq 3$  Å, potentially improving molecular docking approaches that investigate DR ligand selectivity.

The conserved amino acids that create the orthosteric binding pockets (OBPs) of virtually all DR subtypes are well known and described [31,32]. Asp<sup>3.32</sup> in transmembrane (TM) 3 is responsible for ligand recognition forming a salt bridge with the positively charged amine function of ligands. The serine triade consisting of Ser<sup>5.42</sup>, Ser<sup>5.43</sup> and Ser<sup>5.46</sup> positioned in TM5 is important in orienting the respective ligand (especially if a catechol functional group is involved) and considering the ligands' binding affinity. An aromatic microdomain in TM6 includes Trp<sup>6.48</sup>, Phe<sup>6.51</sup> and Phe<sup>6.52</sup> as well as His/Asn<sup>6.55</sup> and is involved in activating the receptor upon interaction with an agonist. Agonist binding induces the so-called 'rotamer toggle switch', a domino-like cascade along TM6 reorienting the named amino acids, eventually triggering receptor activation. Less is known about DR sub-domains or structural elements originating from ligands responsible for selectivity. The D<sub>1</sub>R, although belonging to the D<sub>1</sub>-like DR family, is phylogenetically closest to the  $\beta$ -adrenergic receptors ( $\beta$ ARs) [33]. Consequently, it features distinct motifs, responsible for selectivity. A study by Zhuang et al. suggested the involvement of the extracellular loop (ECL) 2, more specifically Ser188, which enables the D<sub>1</sub>R to accommodate bulkier ligands such as SKF81297 and SKF83959 [34]. In comparison, the same ligands would sterically clash with the corresponding amino acid Ile184 in the ECL2 of the D<sub>2</sub>R, consequently resulting in D<sub>1</sub>R-selectivity over the D<sub>2</sub>-like DR family. Considering selectivity between D<sub>2</sub>R and D<sub>3</sub>R, work by Newman et al. revealed a secondary binding pocket (SBP), consisting of multiple amino acids such as Val<sup>2.61</sup>, Leu<sup>2.64</sup>, Phe<sup>3.28</sup> and conserved Gly and Cys residues located in ECL1 and ECL2, respectively [35]. In more detail, Michino and colleagues have suggested the Gly residue in ECL1 to be the critical selectivity determinant [36]. Additionally, studies have shown that the D<sub>3</sub>R possesses an intrinsically higher affinity towards ligands such as dopamine and quinpirole. Robinson and colleagues have shown that the intracellular loop (ICL) 3 might be responsible for this behaviour. Generating D<sub>2</sub>R hybrids containing the D<sub>3</sub>R-ICL3 motif could increase ligand affinity 10- to 20-fold compared with the wild-type D<sub>2</sub>R. A D<sub>3</sub>R-D<sub>2</sub>R-ICL3 hybrid showed inverse effects [37]. An overview of the described SBP and the different domains involved in DR subtype selectivity is shown in Figure 1.

A great deal of effort has been invested in CADD-approaches to investigate and discover potential DR subtype-selective ligands, thus benefitting drug development in, e.g., neurodegenerative diseases such as PD [28,30,31,34,38,39]. However, due to the complexity of DR selectivity, in silico approaches require in vitro validation. In vitro binding affinities at different DR subtypes can be investigated using, e.g., homogenous time-resolved fluorescence (HTRF) assays, which are standardizable, commercially available and also semi-high-throughput compatible [40,41].

Therefore, the aim of this study was to develop a combined in silico/in vitro approach to assess the selectivity of novel DR ligands at different receptor subtypes using a cell-based HTRF assay as well as a molecular docking approach. Discovering DR-selective ligands as well as providing more detailed insights into their binding behaviour would contribute to better pharmacological tools and new starting points in drug development.

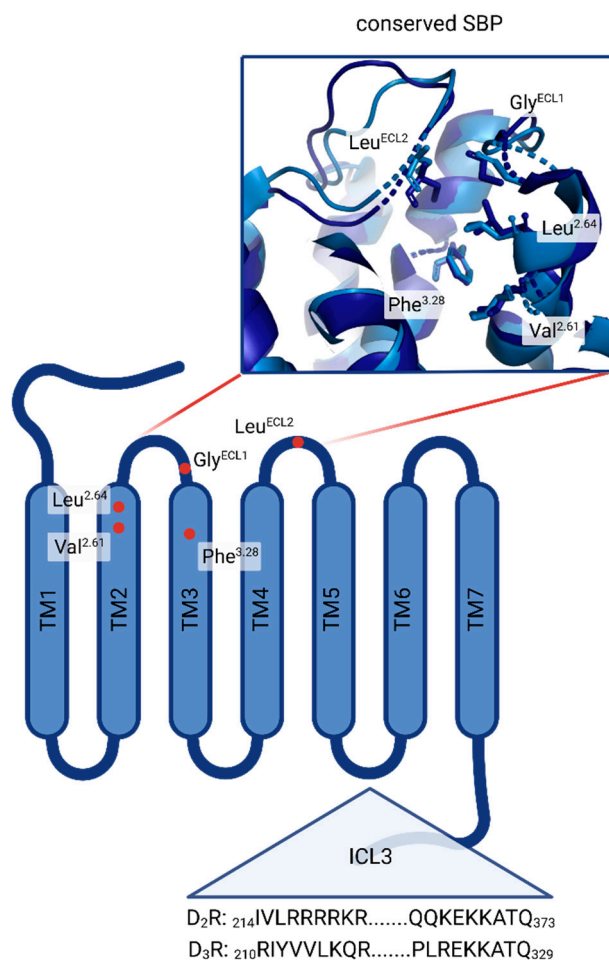


**Figure 1.** Overview of DR sub-domains relevant in DR subtype selectivity. Red dots highlight the highly conserved amino acids Val<sup>2.61</sup>, Leu<sup>2.64</sup>, Phe<sup>3.28</sup>, Gly<sup>ECL1</sup> and Leu<sup>ECL2</sup> in the SBP of D<sub>2</sub>R and D<sub>3</sub>R. Zoomed in box of the conserved SBP shows the 3D arrangement. Partial primary sequences (amino acid positions are shown in the index) of ICL3 are shown for both D<sub>2</sub>R and D<sub>3</sub>R. (Created with BioRender.com (accessed on 13 April 2023)).

## 2. Materials and Methods

### 2.1. Materials

Bromocriptine mesylate (50 mg; CAYM14598-50) was acquired from avantor VWR (Radnor, PA, USA). A68930 hydrochloride (10 mg; A68930) was acquired from biotechne Tocris (Bristol, United Kingdom). Apomorphine hydrochloride was kindly provided by EVERPharma AT GmbH (Unterach, Austria) within the context of a different project. Compounds tested in vitro (shown in Table S5) were acquired either from SPECS (<https://www.specs.net/>, accessed on 30 April 2021) or Maybridge (<https://www.thermofisher.com/at/en/home/industrial/pharma-biopharma/drug-discovery-development/screening-compounds-libraries-hit-identification.html>, accessed on 17 April 2021). All tested compounds were dissolved in 100 % DMSO (dimethyl sulfoxide, acquired from Sigma-Aldrich, St. Louis, MO, USA) and stored at  $-80^{\circ}\text{C}$  until further use.

### 2.2. Ligand Selection for Combined In Silico/In Vitro Approach

Compounds selected for combined in silico/in vitro investigations were chosen based on two main criteria. First, compounds identified as active D<sub>2</sub>R ligands with the previously developed workflow shown in Zell et al. [42] were selected for further in vitro investigations. Second, other compounds from this study showing normalized decreased fluorescence (NDF) values  $\geq 2$ -fold increased (during in vitro activity screening, Section 2.10) at any of

the investigated DR subtypes compared with the other two DR subtypes were included in further investigations.

### 2.3. Similarity Assessment—Tanimoto Scoring (TS) Matrix

Canonical SMILES codes of all the compounds of interest were imported to Canvas version 3.8 (Canvas, Schrödinger Inc., New York, NY, USA). In Canvas version 3.8, radial fingerprints (Extended Connectivity Fingerprint (ECFP4) [43,44]) of all the molecules (based on 2D structures) were calculated followed by an automated calculation of a TS [45] for each compared pair. TS matrices were exported to Excel (Microsoft, Redmond, WA, USA) as csv files and imported to GraphPad Prism version 8 (GraphPad Software, San Diego, CA, USA) to display heatmaps, color-coding the structural similarities. An increasing coefficient indicated an increasing structural similarity. (Dis-)similarities considering chemical scaffolds were further used to assess observed *in silico/in vitro* phenomena.

### 2.4. Dataset Assembly for Molecular Docking (ChEMBL Validation)

For the validation of the molecular docking approach, DR ligands with known biological activities were extracted from the ChEMBL (<https://www.ebi.ac.uk/chembl/> (accessed on 22 April 2022)) for all three DR subtypes investigated *in vitro*. Only entries originating from homo sapiens (UniProt accession numbers: D<sub>1</sub>R, P21728; D<sub>2</sub>R, P14416 and D<sub>3</sub>R, P35462) were considered. ChEMBL entries were only selected for further evaluation if (I) K<sub>i</sub> values for all three DR subtypes were available for each respective molecule and (II) the *in vitro* measurements included a valid control. The curated ChEMBL entries were divided into D<sub>1</sub>R-, D<sub>2</sub>R-, D<sub>2</sub>like- and D<sub>3</sub>R-selective subsets. D<sub>1</sub>R-, D<sub>2</sub>R- or D<sub>3</sub>R-selectivity was assumed for molecules with binding affinities  $\leq 1000$  nM at the respective subtype and  $\geq 1000$  nM at the others. Additionally, the K<sub>i</sub> values were required to differ at least by a factor of two. D<sub>2</sub>like-selective compounds showed binding affinities  $\leq 500$  nM at D<sub>2</sub>R and D<sub>3</sub>R. The final datasets consisting of 29 (SC1–SC29 [46–60]), 25 (SC30–SC54 [53,61–72]), 152 (SC55–SC206 [56,69,72–106]) and 78 (SC207–SC284 [53,56,62,63,65,66,79,87,89,96,99–101,103–118]) molecules, respectively, are shown in Tables S1–S4.

### 2.5. Data Set Preparation for Molecular Docking

All compounds were energetically minimized using the mmFF94 forcefield in OMEGA version 3.0.1.2 prior to molecular docking. (OpenEye Scientific Software, Santa Fe, NM, USA) [119].

### 2.6. Molecular Docking Workflow

Docking was performed using GOLD version 5.8.0 (CCDC, Cambridge, United Kingdom) [120]. Protein structures were not energetically minimized during the docking process. Hydrogens were added to all protein structures. CHEMPLP was used as a scoring function, not allowing early termination. For defining the binding site, all atoms within 6 Å of the bound ligand (depending on the cryo-EM structure) were chosen. The number of GA runs was set to 30.

#### 2.6.1. Molecular Docking—D<sub>1</sub>R

Molecular docking into the D<sub>1</sub>R was performed using the apomorphine-bound cryo-EM structure of the PDB entry 7jvq [34]. Specific settings for the D<sub>1</sub>R structure used during docking are shown in Table 1.



**Table 1.** Summary of the amino acid flexibility settings of the D<sub>1</sub>R cryo-EM structure used during docking.

Setting	Value
Flexible Sidechains	ASP103 R, 1 rotamer (free)
	TRP285 R, 1 rotamer (free)
	PHE288 R, 1 rotamer (free)
	PHE289, 1 rotamer (free)
	ASN292 R, 1 rotamer (free)

### 2.6.2. Molecular Dynamics Simulation (MDS)—D<sub>2</sub>R

Details about the MDS are shown in the supplementary information (Figure S1 and Tables S5–S8). A detailed description of the MDS calculation is given in Tables S5–S8.

### 2.6.3. Molecular Docking D<sub>2</sub>R

Molecular docking into the D<sub>2</sub>R ligand binding site was performed using the MDS-modified (see Section 2.6.2) cryo-EM structure of the PDB entry 7jvr [34]. During docking, only ASP114R was specified as flexible (1 rotamer (free)).

### 2.6.4. Molecular Docking D<sub>3</sub>R

Molecular Docking into the D<sub>3</sub>R was performed using the PD128907-bound cryo-EM structure of the PDB entry 7cmv [121]. Specific settings for the D<sub>3</sub>R structure used during docking are shown in Table 2.

**Table 2.** Summary of the amino acid flexibility settings of the D<sub>3</sub>R cryo-EM structure used during docking.

Setting	Value
Flexible Sidechains	ASP110 R, 1 rotamer (free)
	HIS349 R, 8 rotamers (constrained)

## 2.7. DR Subtypes—BLASTP Alignment

To identify the analogous amino acids of the SBP of D<sub>1</sub>R and D<sub>2</sub>R in respect to D<sub>3</sub>R (defined in [35,36]) a BLASTP alignment was performed (<https://blast.ncbi.nlm.nih.gov> (accessed on 10 March 2023)) [122]. The relevant amino acids in regard to the SBP of D<sub>3</sub>R are shown in Table 3.

**Table 3.** Overview of the amino acids forming the SBP in different DR subtypes. D<sub>2</sub>like subtypes include D<sub>2</sub>R and D<sub>3</sub>R.

D <sub>3</sub> R	DR Subtype D <sub>1</sub> R	D <sub>2</sub> R	Status
Val86	Lys81	Val91	Conserved in D <sub>2</sub> like DRs
Leu89	Ala84	Leu94	Conserved in D <sub>2</sub> like DRs
Gly94	Gly88	Gly98	Conserved
Phe106	Trp99	Phe110	Conserved in D <sub>2</sub> like DRs
Cys181	Cys186	Cys182	Conserved

The respective amino acids were used during the in silico selectivity assessment during the validation process and the analysis of the novel DR ligands.

### 2.8. Validation of the Molecular Docking Approach—ChEMBL Dataset(s)

Molecular docking results for each ChEMBL dataset (containing 30 poses for each compound) were uploaded to Pipeline Pilot Client version 9.1 (Accelrys, San Diego, CA, USA) [123]. Duplicates from each molecular docking output were removed. Only top-ranked poses (based on fitness score) of each docked compound were retained in the datasets used for further evaluation. The subsequent docking analysis (top-ranked poses) was performed using DiscoveryStudio (DS) 2018 Client (Accelrys, San Diego, CA, USA). The (modified) DR subtype protein structures were loaded into DS. The conserved Gly residues (shown in Table 3) were marked; centroids were calculated and checked as center of mass (COM). Subsequently, the docked DR subtype-selective output files were loaded into the respective DR protein structure. All molecules were marked and COM was calculated with respect to the Gly residues. Finally, distances between COM (Gly residue) and COM (docked ligands) were calculated in Å.

### 2.9. Docking Analysis—Novel DR Ligands

The docking analysis of the novel ligands was performed using LigandScout version 4.4.4 (Inte:Ligand GmbH, Vienna, Austria). Docked ligands (sd files) were loaded into the different DR protein structures (D<sub>1</sub>R into 7jvq [34]; D<sub>2</sub>R into the MDS-modified D<sub>2</sub>R 7jvr [34]; and D<sub>3</sub>R into 7cmv [121], respectively). All 30 poses of each ligand were individually superimposed and the most frequent pose was assessed visually. Subsequently, DR protein structures as well as molecular docking output files, were loaded in PyMOL (Schrödinger Inc., New York, NY, USA) for each DR subtype individually. The protein including the most frequent respective ligand pose (taking the highest-ranking according to fitness score) was extracted as a pdb file. The resulting pdb files were loaded into DS for calculating distances [Å], as shown in Section 2.8.

### 2.10. HTRF-Based Receptor Binding Studies

All HTRF assays were performed using an HTRF-compatible plate reader (model Tecan Spark (Tecan Group, Männedorf, Switzerland)). The respective settings were specifically modified and optimized for the determination of D<sub>2</sub>R ligand-binding affinities. Binding affinities were determined using the same settings for measurements with D<sub>1</sub>R and D<sub>3</sub>R carrier cells. Experiments were performed using two different emission wavelengths at 620 (control) and 665 (D<sub>2/3</sub>R)/510 (D<sub>1</sub>R) nm, respectively. Fluorophores were excited at 320 nm. A dichroic 510 mirror was used, while lag and integration times of 100 and 400 µs were applied, respectively. Flashes were set to 75. Electronic gain was automatically optimized, while the z-position was optimized based on the well with the highest expected signal. Experiments described in Sections 2.11, 2.12 and 2.14 required the use of two 96-well plates. The first plate was used to determine the gain and the z-position. Subsequently, the determined values were set manually for the second plate to enable direct comparison between the different plates.

### 2.11. Characterization of DR Carrier Cells (D<sub>1</sub>R and D<sub>3</sub>R)—K<sub>d</sub> Determination

The cells used for the subsequent screening and detailed investigation of D<sub>1</sub>R and D<sub>3</sub>R ligands were acquired from PerkinElmer/cisbio (Waltham, MA, USA; Tag-lite Dopamine D1 or D3a-labeled Cells, ready-to-use (transformed and labeled), 200 tests; C1TT1D1 and C1TT1D3A, respectively). The cells were stored in liquid nitrogen until further use. Fluorescent-labelled ligands (Dopamine D2 Receptor red antagonist Fluorescent Ligand (L0002RED), stored at −20 °C and Dopamine D1 Receptor green antagonist (L0031GRE), stored at −20 °C), assay buffer (5Xconcentrate Tag-lite Buffer (TLB), 100 mL, stored at +4 °C; LABMED), and 96-well plates (HTRF 96-well low-volume white plate; 66PL96005) required for the in vitro assay were also acquired from PerkinElmer/cisbio. The assay was conducted according to the standard operation protocol (SOP) available from PerkinElmer/cisbio. The 96-well plates were incubated at room temperature for 2 h. The 96-well plates were

read as described in Section 2.10. The respective concentrations of the dilution series were performed in triplicates. In total,  $K_d$  determination was performed twice.

The characterization of the  $D_2R$  carrier cells is detailed in [42].

#### 2.12. *In Vitro* Screening—Assessment of Compound Activity

Materials described in Sections 2.1 and 2.11 were also used during ligand screening. TLB (1X was prepared diluting 5X concentrate TLB in water. For ligand screening, compounds were prepared at a working solution concentration of 40  $\mu$ M in 1X TLB. Compound 1, apomorphine, was used as the positive control at the same concentration. The assay was conducted in duplicates following the SOP available from PerkinElmer/cisbio and as described in Section 2.10.

#### 2.13. Ligand Selection for $K_i$ Determination

Ligand selection was based on NDF values detailed in Table S9. Novel  $D_2R$  ligands from our previous study (compounds 2, 3, 5, 6, 7 and 9) [42] were selected for selectivity assessment. Additionally, compounds 4, 8 and 10 were investigated due to an NDF fold-difference  $\geq 2$  of any of the three DR subtypes compared with the other two.

#### 2.14. $K_i$ Determination for Selected Ligands

The materials described in 2.1 and 2.11 were also used for  $K_i$  determination of the ligands selected after screening. The selected ligands (compounds 1–10) were diluted in 1x TLB. Compounds 1, 2 and 4–9 were diluted to an initial working solution concentration of  $4 \times 10^{-4}$  M. Compounds 3 and 10 were diluted to an initial working solution concentration of  $1 \times 10^{-4}$  M. Different concentrations were chosen due to differences in aqueous solubility of the compounds. The  $K_i$  was determined in duplicates following the SOP available from PerkinElmer/cisbio and as described in Section 2.10.

#### 2.15. Data Processing, Representation and Analysis

Saturation binding curves were processed and visualized in GraphPad Prism 8 (Non-linear regression (curve fit), One site—Fit  $\log IC_{50}$  was performed using GraphPad Prism version 8.2.1 for Windows, GraphPad Software, San Diego, CA, USA). Molecular docking was performed in GOLD 5.8.0 (CCDC, Cambridge, United Kingdom) [120]. Docking analysis was performed in LigandScout version 4.4.5 (Inte:Ligand GmbH, Vienna, Austria) [124]. MDS and calculations for distance-based in silico approach were performed in DS Client 2018 (DiscoveryStudio, Accelrys Inc., San Diego, CA, USA). Two-dimensional structures of all shown compounds were generated using ChemDraw version 19.0 (PerkinElmer, Waltham, MA, USA). SD files used for similarity assessment were generated using PipelinePilot Client 9.1 (Dassault Systems, BIOVIA Discovery Studio, San Diego, CA, USA, 2018). Similarity assessment was performed using Canvas 3.8 (Canvas, Schrödinger, LLC, New York, NY, USA, 2021). Docking alignments and visualization were performed in PyMOL (PyMOL, Schrödinger, LLC, New York, NY, USA, 2021).

### 3. Results

#### 3.1. Structural Summary of the Investigated Ligands

All compounds investigated in silico and in vitro within this study are shown in Figure 2.

The novel ligands (compounds 2–10) investigated with the combined approach within the scope of this study were structurally compared with each other using a Tanimoto scoring (TS) matrix. Therefore, the observed in silico and/or in vitro phenomena could be potentially correlated to structural (dis-)similarities. The TS matrix is shown in Figure 3, ranging from 0 (green) to 1 (red), corresponding to structurally unrelated and identical compounds, respectively.



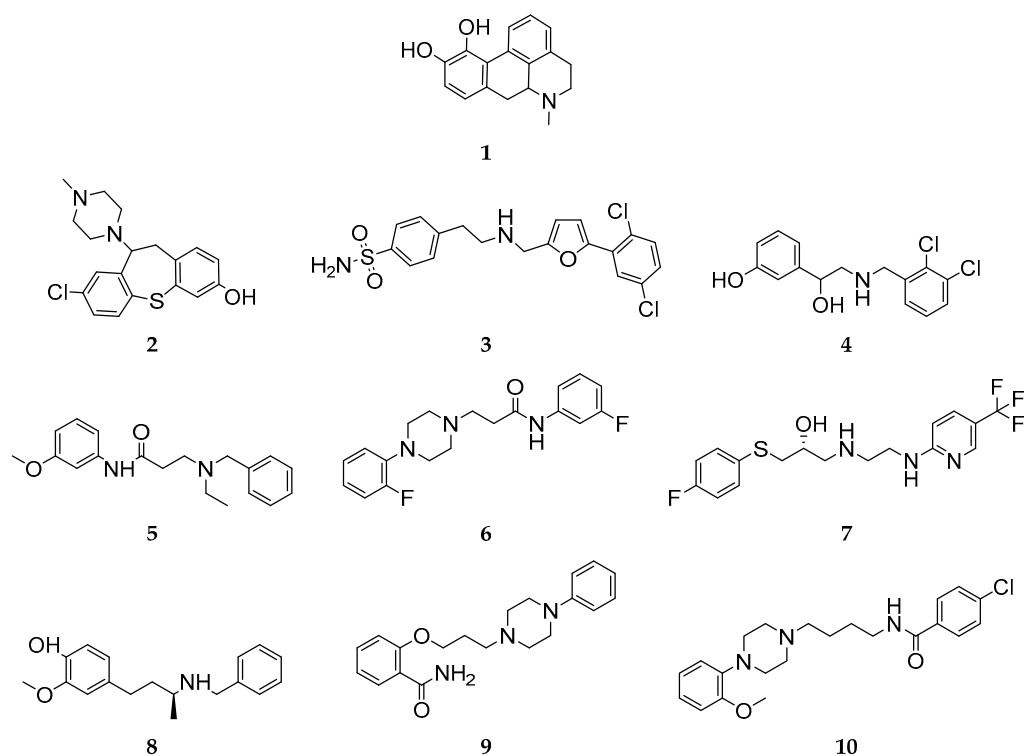


**Figure 2.** Overview of the 2D structures of ligands investigated in silico and in vitro.

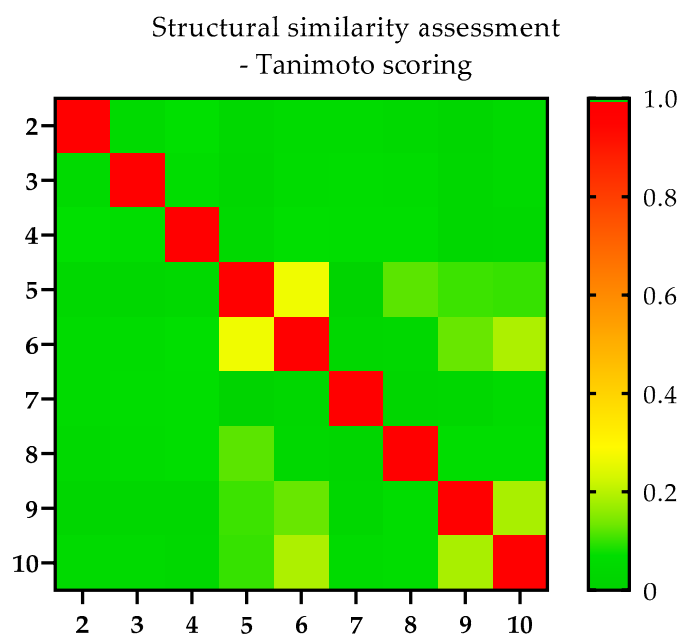


**Figure 3.** Overview of the structural (dis-)similarity of the investigated novel ligands (compounds 2–10). (Dis-)similarity was assessed utilizing a TS matrix based on radial fingerprints (ECFP4). TS ranging from 0 (green) to 1 (red) showing unrelated and identical structures, respectively. Numbers given on the *x*- and *y*-axis indicate the different compounds investigated within this study.

Thirty-three out of thirty-six pairs scored between 0.03 and 0.15, thus representing a structurally diverse compound collection. Only three pairs, i.e., compounds 5 and 6 (TS 0.28), 6 and 10 (TS 0.21) and 9 and 10 (TS 0.21), were characterized by a similarity score of >0.21, reflecting a higher degree of similarity (considering the use of radial fingerprints).

### 3.2. In Vitro Compound Screening—An Assessment of DR Subtype Selectivity

The investigated compounds were taken from a previous pharmacophore-based virtual screening study described in Zell et al. [42]. All 2D structures (compounds **2–10** and **SC285–SC365**) and respective NDF values for all DR subtypes are shown in Table S9 and Figures S2–S10. The activities of all compounds were investigated via a competitive binding (in comparison with a fluorescence-labeled ligand) of the respective compounds at D<sub>1</sub>R/D<sub>3</sub>R, utilizing an HTRF assay using a screening concentration of 10 μM. NDF values of compounds chosen for further evaluation are shown in Table 4.

**Table 4.** Summary of the in vitro screening of known and potential DR ligands considered selective for one of the three investigated subtypes. All measurements were conducted at a concentration of 10 μM (*n* = 4). Fluorescence decrease was normalized to the control. Cpd., compound.

Cpd.	Normalized Decrease in Fluorescence (NDF) ± SD		
	D <sub>1</sub> R	D <sub>2</sub> R <sup>a</sup>	D <sub>3</sub> R
Control	1	1	1
<b>1</b>	3.47 ± 1.04	9.44 ± 5.97	3.82 ± 1.32
<b>2</b>	5.46 ± 1.97	40.41 ± 1.39	4.16 ± 1.08
<b>3</b>	1.78 ± 1.35	3.99 ± 2.58	3.96 ± 1.10
<b>4</b>	0.90 ± 0.31	0.90 ± 0.39	2.75 ± 0.61
<b>5</b>	1.26 ± 0.64	15.74 ± 18.15	2.65 ± 0.64
<b>6</b>	2.15 ± 1.16	8.18 ± 3.62	4.21 ± 0.79
<b>7</b>	1.57 ± 0.54	10.85 ± 4.93	3.79 ± 0.70
<b>8</b>	1.20 ± 0.59	1.10 ± 0.52	2.63 ± 0.52
<b>9</b>	1.71 ± 0.86	22.08 ± 6.62	3.97 ± 0.78
<b>10</b>	2.59 ± 1.04	22.89 ± 8.41	4.09 ± 1.07

<sup>a</sup> Values were extracted from previous experiments detailed in [42].

Based on the resulting NDF values, all compounds but **4** and **8** showed promiscuous receptor activities suggesting diverse selectivity profiles. Only compounds **4** and **8** showed NDF values close to 1 at both D<sub>1</sub>R and D<sub>2</sub>R, suggesting inactivity at those DR subtypes and, respectively, selectivity for the D<sub>3</sub>R.

### 3.3. Ki Determination—Of the Selected Compounds at DR Subtypes

The selected compounds were investigated in vitro to determine their binding affinities (K<sub>i</sub> values) at the three different DR subtypes, D<sub>1</sub>R, D<sub>2</sub>R and D<sub>3</sub>R. In Figure 4a,b, compounds **2** and **10** are shown as examples. Compound **2** represents a non-selective ligand while compound **10** is characterized by the highest selectivity (for D<sub>3</sub>R). The remaining binding curves are shown in Figure S11a–h.

The K<sub>i</sub> values of all investigated ligands, as well as the calculated fold-differences for each receptor pair, are shown in Table 5.

All the compounds investigated in vitro, except compound **1**, showed a clear D<sub>2</sub>like selectivity with preferences for D<sub>3</sub>R (D<sub>1</sub>R/D<sub>3</sub>R fold differences ranging from 3.06 to 1031.4, D<sub>2</sub>R/D<sub>3</sub>R fold-differences ranging from 1.66 to 263.7, respectively). While compounds **2**, **5**, **6**, **9** and **10** showed higher affinities for D<sub>1</sub>R compared with the D<sub>2</sub>like DR subtypes, the affinities of compounds **3**, **4** and **8** were not determinable for D<sub>1</sub>R, and were thus considered inactive. Compounds **4** and **8** were also inactive at D<sub>2</sub>R, and were thus considered D<sub>3</sub>R-selective. Only compound **1** was characterized by the lowest binding affinity for D<sub>2</sub>R. Interestingly, all compounds showed the highest affinity at the D<sub>3</sub>R.

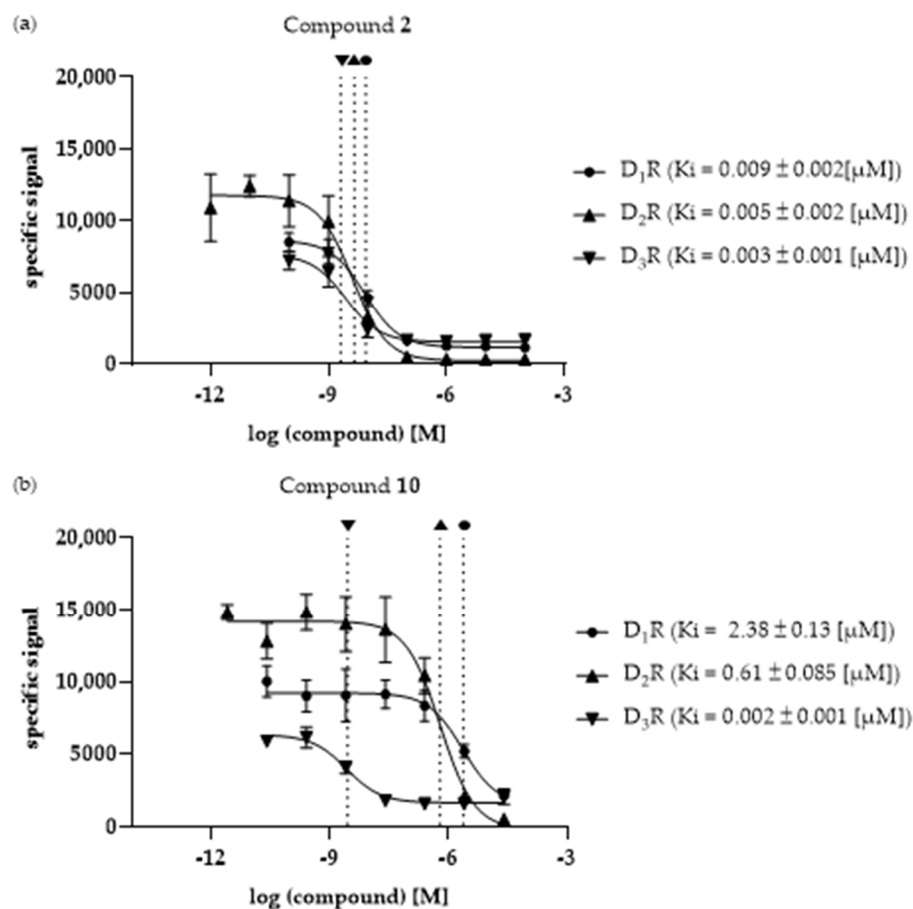


**Figure 4.** Comparison of the  $K_i$  values of compounds (a) 2 and (b) 10 determined at the investigated DR subtypes  $D_1R$ ,  $D_2R$  and  $D_3R$ . Vertical, dotted lines indicate the respective  $K_i$  values at the different DR subtypes.  $K_i$  values [ $\mu\text{M}$ ]  $\pm$  SD were determined with  $n = 6$ .

**Table 5.** Summary of the determined  $K_i$  values of all ligands investigated in vitro. Binding affinities are shown for the three different DR subtypes  $D_1R$ ,  $D_2R$  and  $D_3R$ .  $K_i$  values were determined using  $n = 6$ . Apomorphine (1) was used as a control. Cpd., compound.

Cpd.	Ki [ $\mu\text{M}$ ]			Selectivity		
	$D_1R$	$D_2R$	$D_3R$	$D_1R/D_2R$	$D_1R/D_3R$	$D_2R/D_3R$
1	$0.36 \pm 0.009$	$2.36 \pm 0.14$	$0.12 \pm 0.048$	0.15	3.06	19.8
2	$0.009 \pm 0.002$	$0.005 \pm 0.002^a$	$0.003 \pm 0.001$	1.95	3.23	1.66
3	n.d. <sup>b</sup>	$4.66 \pm 2.69^a$	$0.38 \pm 0.022$	$>21.4^b$	262.2	12.2
4	n.d. <sup>b</sup>	n.d. <sup>b</sup>	$3.68 \pm 0.94$	-	$>27.2^b$	$>27.2^b$
5	$46.9 \pm 27.4$	$10.95 \pm 4.43^a$	$2.25 \pm 0.91$	4.28	20.8	4.86
6	$7.76 \pm 4.41$	$1.35 \pm 0.63^a$	$0.37 \pm 0.28$	5.77	20.7	3.56
7	$8.33 \pm 2.17$	$2.78 \pm 1.06^a$	$0.68 \pm 0.068$	3.00	12.3	4.11
8	n.d. <sup>b</sup>	n.d. <sup>b</sup>	$2.32 \pm 0.92$	-	$>43.1^b$	$>43.1^b$
9	$9.46 \pm 1.18$	$0.33 \pm 0.093^a$	$0.024 \pm 0.003$	28.6	395.1	13.8
10	$2.38 \pm 0.13$	$0.61 \pm 0.085$	$0.002 \pm 0.001$	3.91	1031.4	263.7

<sup>a</sup> Values were extracted from previous experiments detailed in [42]. <sup>b</sup>  $K_i$  values could not be quantitatively determined. To calculate values for selectivity,  $K_i$  values were assumed to be  $\geq 100 \mu\text{M}$  (highest concentration used during in vitro testing). n.d., not determinable.

### 3.4. Dataset Assembly—*In Silico* Assessment

To validate the molecular docking approach utilized to assess compound selectivity *in silico*, DR ligands with different selectivities for the DR subtypes D<sub>1</sub>R, D<sub>2</sub>R and D<sub>3</sub>R with known biological activities were extracted from the ChEMBL database. Compounds were only included in the final datasets if (I) their binding affinities were determined *in vitro* at all three DR subtypes and (II) their *in vitro* measurements included a valid control to assess assay functionality. The curated ChEMBL entries were divided into D<sub>1</sub>R-, D<sub>2</sub>R-, D<sub>2</sub>like- and D<sub>3</sub>R-selective subsets. D<sub>1</sub>R-, D<sub>2</sub>R- or D<sub>3</sub>R-selectivity was assumed for molecules with binding affinities  $\leq 1000$  nM at the respective subtype and  $\geq 1000$  nM at the others. D<sub>2</sub>like-selective compounds showed binding affinities  $\leq 500$  nM at D<sub>2</sub>R and D<sub>3</sub>R. The final datasets consisting of 29 (SC1–SC29 [46–60]), 25 (SC30–SC54 [53,61–72]), 152 (SC55–SC206 [56,69,72–106]) and 78 (SC207–SC284 [53,56,62,63,65,66,79,87,89,96,99–101,103–118]) molecules, respectively, are shown in Table S1 to Table S4.

### 3.5. Validation of Molecular Docking

The utilized molecular docking approach was based on the work of Michino and colleagues [36]. Therefore, different ChEMBL datasets, previously defined as DR subtype-selective (see Section 3.4), were docked into the 3D protein structures of D<sub>1</sub>R, D<sub>2</sub>R and D<sub>3</sub>R (molecular docking workflow described in Sections 2.6.1, 2.6.3 and 2.6.4). Due to the high number of investigated ligands (>300), only the top-ranked poses (considering the fitness score) were considered during further analysis. The COM for all ligands included in each specific DR-selective subset was calculated using DS. Distances of each COM with respect to each DRs conserved Gly residue (shown in Table 3) were calculated in [Å]. The calculated fold-differences for each subset, comparing different DRs with each other, are shown in Figure 5 (absolute distances determined in DS are given in Table S10).

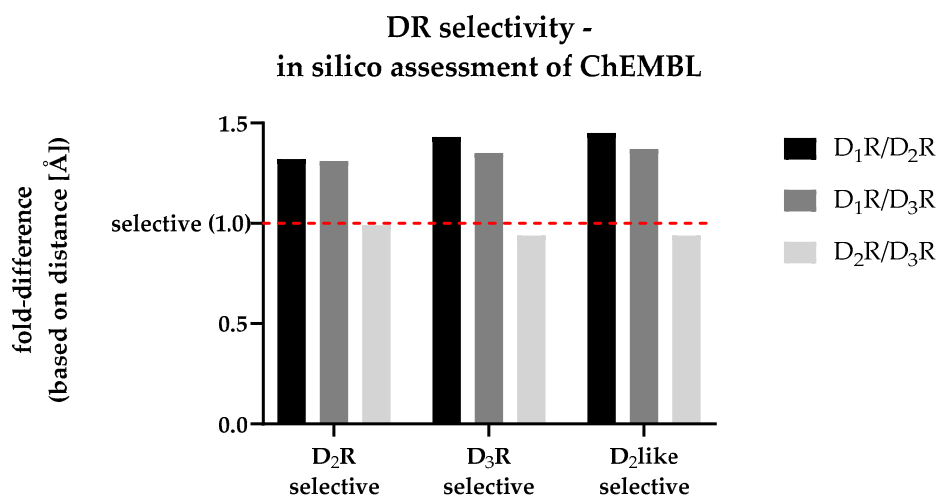


**Figure 5.** Comparison of the fold-differences based on the distances [Å] between each DR-selective subsets COM and the respective conserved Gly residue. The dashed red line shows a distance-based fold-difference of 1.0, indicating a non-selective profile of the respective dataset based on the *in silico* analysis.

The dashed red line shown in Figure 6 indicates a fold-difference of 1.0, which indicates the same distance between the ligands collective COM and the conserved Gly residue after docking into the respective DR structures. All investigated datasets show a fold-difference close to 1.0 considering the D<sub>2</sub>R/D<sub>3</sub>R comparison. This means that they showed an almost identical distance between COM and the Gly residue. In contrast, all datasets showed an increased fold-difference  $> 1.0$ , when comparing D<sub>1</sub>R with D<sub>2</sub>R or D<sub>3</sub>R, respectively. Details considering all datasets are shown in Table 6.

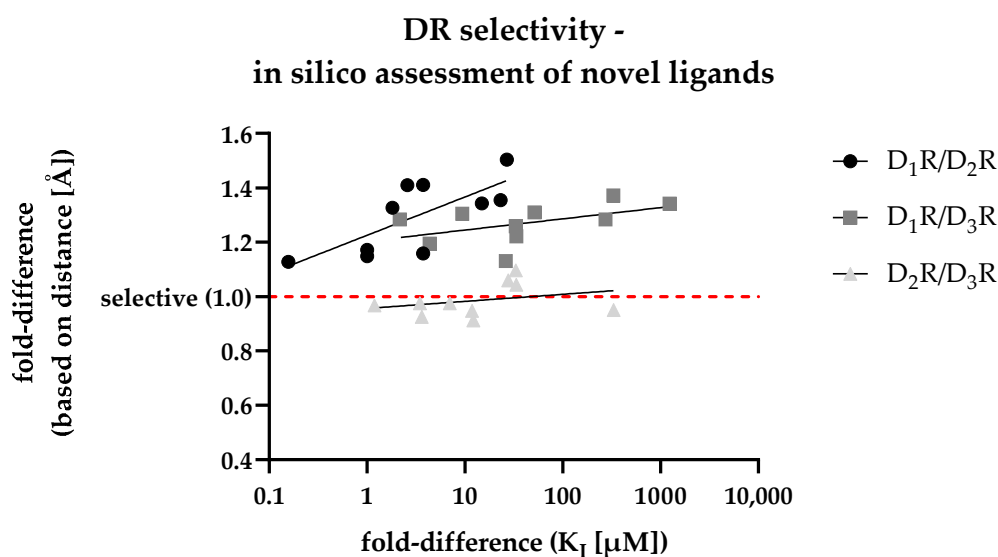


**Figure 6.** Correlation of in vitro determined fold-differences ( $x$ -axis) and in silico determined distance-based fold-differences ( $y$ -axis) to investigate DR subtype selectivity of novel compounds. The dashed red line shows a distance-based fold-difference of 1.0, indicating a non-selective profile of the respective compound based on the in silico analysis.

**Table 6.** Summary of the distance-based docking approach of different DR-subtype selective ChEMBL datasets. Calculated fold-differences were based on distances [Å] between COM and the respective conserved Gly residue.

Dataset	Fold-Difference (Cons. Gly-COM)		
	D <sub>1</sub> R/D <sub>2</sub> R	D <sub>1</sub> R/D <sub>3</sub> R	D <sub>2</sub> R/D <sub>3</sub> R
D <sub>2</sub> R selective	1.32	1.31	0.99
D <sub>3</sub> R selective	1.43	1.35	0.94
D <sub>2</sub> like selective	1.45	1.37	0.94

Clearly, the approach was incapable of distinguishing D<sub>2</sub>R- and D<sub>3</sub>R-selectivity from each other based on the COM–Gly distance. However, the utilized molecular docking approach was capable of identifying D<sub>2</sub>like-selective ligands based on their position within the respective DRs OBP.

### 3.6. In Silico Assessment of DR Selectivity—Interaction with the SBP

For the in silico assessment of the selected compounds 1–10, the most frequent poses after docking were used. After calculating the fold-differences based on the distances between each ligand’s individual COM and the respective Gly residue (within each of the three DR subtypes SBP, shown in Table S11), they were plotted against the fold-differences based on the DR-specific  $K_i$  values (shown in Table 5) determined in vitro. The resulting scatter plot is shown in Figure 6.

In addition to the individual data points, Figure 6 shows regression curves for all DR pairs. The D<sub>1</sub>R/D<sub>2</sub>R curve (dots) was characterized by the steepest slope suggesting the capability of the in silico approach in discriminating D<sub>2</sub>R-selective ligands. While the slope for the D<sub>1</sub>R/D<sub>3</sub>R curve (squares) was less steep, the calculated fold-differences (based on distance,  $y$ -axis) was already higher at lower  $K_i$ -based fold-differences ( $x$ -axis), indicating a similar capability to discriminate D<sub>3</sub>R-selective ligands. The D<sub>2</sub>R/D<sub>3</sub>R curve (triangles) was flatter, with individual values scattered around 1.0. Consequently, this reflected the results shown in Figure 5, where D<sub>2</sub>R/D<sub>3</sub>R-selectivity could not be discriminated based on the selected approach. In summary, the developed distance-based in silico approach was



highly capable in identifying D<sub>2</sub>like-selectivity. This was also indicated by the R<sup>2</sup> values (shown in Figure 6) regarding the D<sub>1</sub>R/D<sub>2</sub>R and the D<sub>1</sub>R/D<sub>3</sub>R comparison showing a positive correlation between increasing binding affinities with increasing selectivity.

### 3.7. Retrospective Analysis of the In Silico/In Vitro Correlation

To get a more detailed insight into the binding mode of each of the investigated ligands at the respective DR subtype, the most frequent docking poses of each compound (Figures 7–9 and S12–S17) were visualized in the different binding pockets using PyMOL. Figures 7 and 8 show the different binding poses of the non-selective compound 2 and compound 10, which had the highest D<sub>3</sub>R-selectivity.

In Figure 7, the tertiary amine functionality (contained in the piperazine motif) of compound 2 is clearly oriented towards the OBP, allowing the formation of the salt-bridge with Asp<sup>3.32</sup> (described as the crucial interaction to define a DR ligand). While the position of compound 2 was flipped in D<sub>2</sub>R in comparison with D<sub>1</sub>R and D<sub>3</sub>R (highlighted by the orientation of the chlorine, green), the overall positioning of compound 2 was similar in each DR subtype. Consequently, there was no distinct orientation of any of the poses towards the SBP, resulting in the non-selective binding with Ki fold-differences between 1.2 and 2.2 (see Table 5).

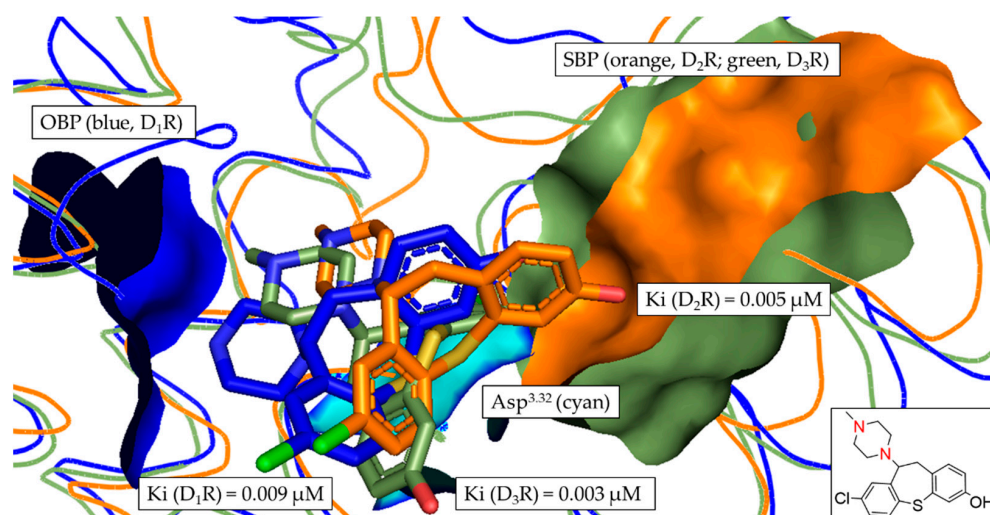


**Figure 7.** Alignment of the most frequent poses of compound 2 docked into D<sub>1</sub>R, D<sub>2</sub>R and D<sub>3</sub>R. The surface of the highly conserved OBP is shown in blue (based on D<sub>1</sub>R) consisting of Asp<sup>3.32</sup> (highlighted in cyan) and Ser<sup>5.42/5.43/5.46</sup>. The conserved SBP-surface is displayed in orange (D<sub>2</sub>R) and green (D<sub>3</sub>R) consisting of Val<sup>2.61</sup>, Leu<sup>2.64</sup>, Gly<sup>EL1</sup>, Phe<sup>3.28</sup> and Cys<sup>EL2</sup> (individual amino acid labels shown in Table 3), respectively. Ki values determined in vitro are shown for each DR subtype. Two-dimensional structure of compound 2 is shown. Amine functional group involved in formation of the salt-bridge is highlighted in red.

In Figure 8, the tertiary amine functionality (contained in the piperazine motif) of compound 10 was again oriented towards the OBP. Thus, the salt-bridge formation with Asp<sup>3.32</sup> was possible. In contrast to compound 2, the binding poses of compound 10 were distinctly different in the respective DR subtypes. Comparing the poses in D<sub>1</sub>R and D<sub>3</sub>R, the D<sub>3</sub>R pose (green) was shifted slightly to the right towards the SBP. The D<sub>2</sub>R binding pose (orange) was clearly different from both D<sub>1</sub>R and D<sub>3</sub>R, with the chloro-substituted ring clearly oriented towards the SBP. While this explained the observed D<sub>1</sub>R/D<sub>2</sub>R fold difference of 3.7, it did not correlate with the D<sub>2</sub>R/D<sub>3</sub>R fold-difference of 331.8. However, the detailed analysis of the binding poses of compound 10 correlated with the observed D<sub>2</sub>like selectivity determined in vitro. Additionally, it also partially confirmed the retrospective results of the distance-based approach shown Figure 6, highlighting the capability of the developed approach to identify D<sub>2</sub>like-selectivity.

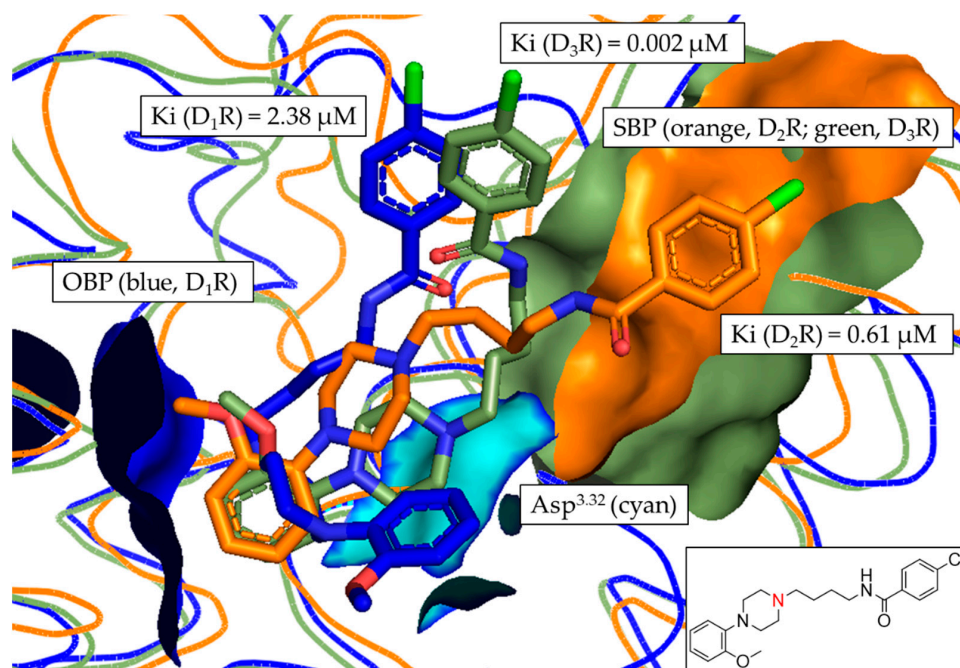


**Figure 8.** Alignment of the most frequent poses of compound 10 docked into D<sub>1</sub>R, D<sub>2</sub>R and D<sub>3</sub>R. The surface of the highly conserved OBP is shown in blue (based on D<sub>1</sub>R) consisting of Asp<sup>3.32</sup> (highlighted in cyan) and Ser<sup>5.42/5.43/5.46</sup>. The conserved SBP-surface is displayed in orange (D<sub>2</sub>R) and green (D<sub>3</sub>R) consisting of Val<sup>2.61</sup>, Leu<sup>2.64</sup>, Gly<sup>EL1</sup>, Phe<sup>3.28</sup> and Cys<sup>EL2</sup> (individual amino acid labels shown in Table 3), respectively. Ki values determined in vitro are shown for each DR subtype. Two-dimensional structure of compound 10 is shown. Amine functional group involved in formation of the salt-bridge is highlighted in red.

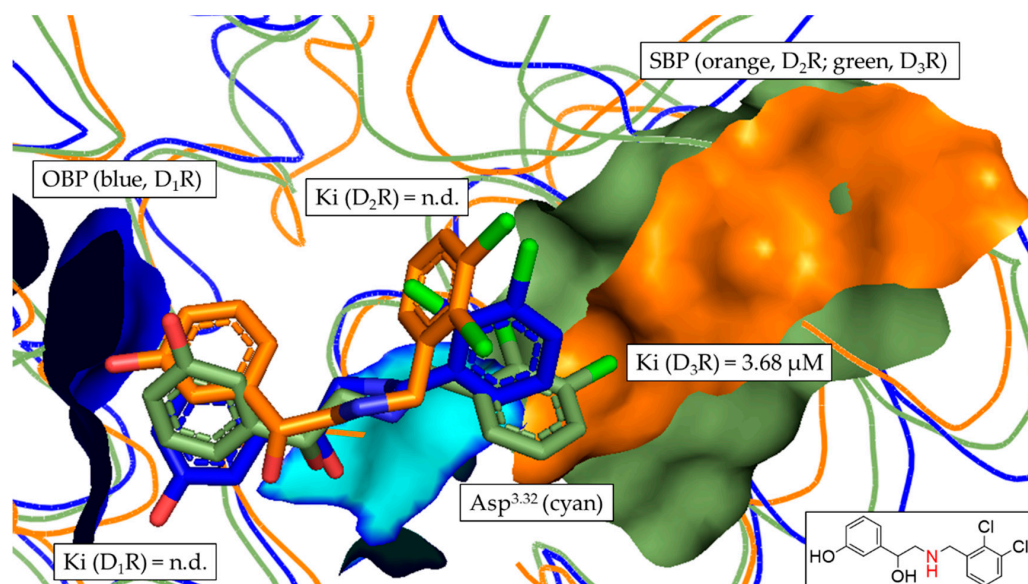


**Figure 9.** Alignment of the most frequent poses of compound 4 docked into D<sub>1</sub>R, D<sub>2</sub>R and D<sub>3</sub>R. The surface of the highly conserved OBP is shown in blue (based on D<sub>1</sub>R) consisting of Asp<sup>3.32</sup> (highlighted in cyan) and Ser<sup>5.42/5.43/5.46</sup>. The conserved SBP-surface is displayed in orange (D<sub>2</sub>R) and green (D<sub>3</sub>R) consisting of Val<sup>2.61</sup>, Leu<sup>2.64</sup>, Gly<sup>EL1</sup>, Phe<sup>3.28</sup> and Cys<sup>EL2</sup> (individual amino acid labels shown in Table 3), respectively. Ki values determined in vitro are shown for each DR subtype. Two-dimensional structure of compound 4 is shown. Amine functional group involved in formation of the salt-bridge is highlighted in red. n.d., not determinable.

These findings were also supported by the in-depth analyses of compounds **3**, **5**, **6**, **7** and **9** (PyMOL alignments shown in Figures S12–S15 and S17), where D<sub>2</sub>R and D<sub>3</sub>R poses were distinctly oriented towards the SBP. However, in agreement with the findings considering compound **10**, the D<sub>2</sub>R- and D<sub>3</sub>R binding poses did not correlate with the higher D<sub>3</sub>R binding affinities found *in vitro*. Again, the results allowed for the confirmation of D<sub>2</sub>like-selectivity of the investigated ligands.

Compounds **4** (Figure 9) and **8** (Figure S16) were the only compounds with no determinable binding affinity at D<sub>1</sub>R and D<sub>2</sub>R, additionally showing slightly increased distance-based fold-differences (Figure 6 and Table S11), regarding D<sub>2</sub>R/D<sub>3</sub>R-selectivity, of 1.10 and 1.04, respectively.

This was also reflected in the binding pose of compound **4**, where the D<sub>3</sub>R pose (green) was oriented closer to the SBP. Similar results were observed in the binding pocket comparison of compound **8**.

#### 4. Discussion

The characterized DR ligands showed different selectivity profiles. Interestingly, all ten compounds investigated by the developed *in silico/in vitro* approach (including the novel compounds **2–10**) showed either D<sub>3</sub>R-preferences or clear D<sub>3</sub>R-selectivity. Compound **2**, for example, showed fold-differences of 3.23 and 1.66 for D<sub>1</sub>R/D<sub>3</sub>R and D<sub>2</sub>R/D<sub>3</sub>R, respectively, thus exerting D<sub>3</sub>R-preferences. Compounds **4** and **8** were characterized by no determinable binding affinities at D<sub>1</sub>R and D<sub>2</sub>R, consequently they were categorized as D<sub>3</sub>R-selective. While compound **10** showed low to intermediate binding affinities at D<sub>1</sub>R (2.38 μM) and D<sub>2</sub>R (0.61 μM), it also exerted the highest quantifiable selectivity fold-differences with values of 1031.4 and 263.7 for D<sub>1</sub>R/D<sub>3</sub>R and D<sub>2</sub>R/D<sub>3</sub>R, respectively. Additionally, all investigated compounds but **1** were D<sub>2</sub>like-selective.

The rather promiscuous behavior of compound **2** is attributed to its structural similarity to clozapine, the prototypical representative of atypical antipsychotics (a drug class belonging to the atypical antipsychotics). While clozapine is characterized by its potent antipsychotic effect, it is also known as a so-called ‘dirty drug’ due to its promiscuous activity at a variety of aminergic GPCRs (including dopaminergic, serotonergic and adrenergic receptor families) [125]. Thus, a similar pharmacological profile of compound **2** was expected. This was not only confirmed by the *in vitro* data but also by the developed *in silico* approach, correlating the positioning of the ligand within the OBP and SBP with its respective DR subtype selectivity. Even though the binding behavior of compound **2** appeared non-selective, the *in silico* approach was capable of detecting the slight D<sub>2</sub>like-preference resulting in distance-based fold-differences of 1.33 and 1.28 for D<sub>1</sub>R/D<sub>2</sub>R and D<sub>1</sub>R/D<sub>3</sub>R, respectively. Moreover, the compound could be active at other GPCRs which were not investigated within this study. In general, the investigated compounds could be biologically active at other PCRs. For example, a study by Garcia-Romero and colleagues identified several antiparkinsonian molecules with polypharmacological profiles. Those molecules were also biologically active at other GPCRs such as muscarinic acetyl choline receptors and adenosine receptors but also at the norepinephrine transporter [126]. This study highlights the necessity of investigating the identified ligands in even more detail to potentially exploit potential polypharmacological aspects and, even more importantly, to identify possible off-target activities. However, this study deliberately focused on isolated ligand–receptor interactions to generate reliable *in silico/in vitro* correlation, thus elaborating upon DR selectivity mechanisms.

The comparison of compounds **6** and **10** allowed for very interesting insights into the DR subtype-selectivity profile of structurally similar ligands differing mainly regarding linker lengths. Compounds **6** and **10** are both characterized by two terminal aromatic rings and a linker region consisting of a piperazine motif, an amide functionality and an alkyl chain (see Figure 2). Moreover, they also share binding preferences at the different DR subtypes following D<sub>1</sub>R > D<sub>2</sub>R > D<sub>3</sub>R. Both compounds showed comparable K<sub>i</sub>-based fold-differences of 5.77 (compound **6**) and 3.91 (compound **10**) for D<sub>1</sub>R/D<sub>2</sub>R. However, the



D<sub>1</sub>R/D<sub>3</sub>R and D<sub>2</sub>R/D<sub>3</sub>R fold-differences increased drastically for compound **10** (1031.4 and 263.7, respectively) compared with compound **6** (20.7 and 3.59, respectively). Michino and colleagues showed similar phenomena in their study investigating the impact of the linker length in analogues of the highly D<sub>3</sub>R-selective compound R22 ([*(R)*-N-(4-(4-(2,3-dichlorophenyl)piperazin-1-yl)-3-hydroxybutyl)-1H-indole-2-carboxamide]) [36,79]. The investigated R-22 analogues included C3- to C5-linker regions. The C3-linker length resulted in non-selective binding behavior at D<sub>2</sub>R and D<sub>3</sub>R. The C5-linker length markedly reduced D<sub>2</sub>R/D<sub>3</sub>R selectivity. Only the C4 analogue retained a significant D<sub>2</sub>R/D<sub>3</sub>R-selectivity with a 45.7 fold-difference. Compound **6**, including a C2-linker region, showed a comparably reduced D<sub>2</sub>R/D<sub>3</sub>R-selectivity of 3.59. In contrast, compound **10**, including a C4-linker region, exerted a fold-difference of 263.7. While compounds **6** and **10** are only partially related (similarities shown in red) to the R22-analogues (see Figure 10), the observed in vitro effects are potentially attributable to the length of the linker region.

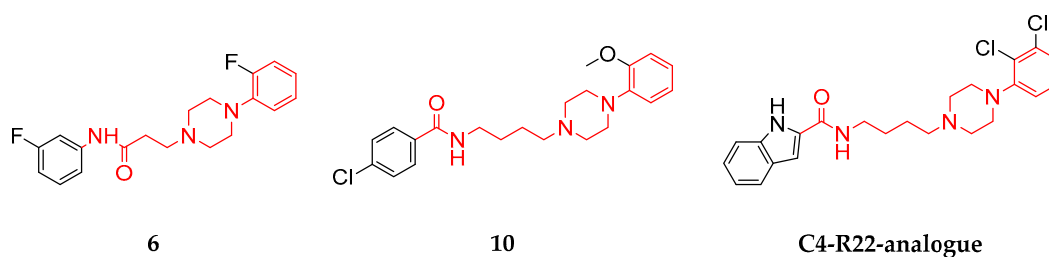


**Figure 10.** Comparison of the chemical scaffolds of compounds **6**, **10** and the R22-analogue. Structural elements highlighted in red show similarities between the different compounds also indicating the differences in linker length.

Compounds **2**, **3**, **5**, **6**, **7** and **9** were already reviewed in our earlier publication investigating their novelty, as was the DR-associated effects of their closest structural relatives [42]. While none of the investigated structures yielded exact structural matches, the most similar structures were associated with different DR-related effects. Structurally similar compounds to **5** and **6** were associated with D<sub>4</sub>R-selectivity but no defined mode of action (agonism or antagonism) [127]. A compound similar to **2** was associated with D<sub>4</sub>R antagonism, while structurally similar ligands regarding compounds **3** and **7** were investigated considering D<sub>2</sub>R antagonism [128–131]. Only a compound structurally similar to **9** was associated with D<sub>3</sub>R-selectivity and D<sub>2</sub>R antagonism [132]. The novel ligands included within this study were compared with the literature using SwissTargetPrediction (<http://www.swisstargetprediction.ch/> (accessed on 5 March 2023)) and SwissSimilarity (<http://www.swissimilarity.ch/> (accessed on 5 March 2023)) [133–135]. Compounds **4** and **8** yielded low scores in SwissTargetPrediction where the identified similar compounds (ChEMBL IDs 59603 and 592377) had been investigated considering D<sub>1</sub>R- and D<sub>2</sub>R activity but not D<sub>3</sub>R selectivity [136,137]. ChEMBL entry 4081151 was structurally closely related to compound **4** but had only been investigated for kappa opioid receptors [138]. A SwissSimilarity match for compound **8** (ChEMBL ID 1094101) was investigated for its binding affinity at serotonergic receptors and aminergic GPCR family members, but not in respect to DRs [139]. Thus, compounds **4** and **8** open up novel insights into D<sub>3</sub>R-selectivity. Compound **10** resulted in exact structural matches and closely related matches in both SwissTargetPrediction and SwissSimilarity investigating D<sub>3</sub>R-selectivity. Still, the comparison between compounds **6** and **10** contributes to a better understanding of the role of the linker length on the DR subtype selectivity of structurally related, but not identical, chemical scaffolds.

As mentioned earlier, all novel ligands exerted their highest binding affinities at the D<sub>3</sub>R. This is partially in accordance with the scientific literature, where the D<sub>3</sub>R shows a high intrinsic binding affinity for agonists such as dopamine (420-fold increased affinity) and quinpirole [37,140]. While this is attributed to intracellular loop 3 in D<sub>3</sub>R, this characteristic has only been shown for agonists. However, the known characteristics of the structurally

related compounds of the novel compounds described above suggest a low probability that all investigated ligands are actually agonists. Thus, the increased D<sub>3</sub>R affinity of compounds 2–10 presumably originates from a distinct interaction with the described SBP [36]. The developed in silico approach proposes a workflow to identify D<sub>2</sub>like-selectivity. However, the static nature of the molecular docking approach does not allow for discrimination of D<sub>2</sub>R/D<sub>3</sub>R-selectivity. This limitation can be attributed to the very dynamic nature of the EL structural motifs of the D<sub>2</sub>like DRs responsible for subtype selectivity. Different studies propose MDS approaches to circumvent the shortcomings of molecular docking approaches and to account for protein flexibility [36,141].

Thus, the developed in silico/in vitro workflow clearly demonstrated its potential use in preclinical drug research by enabling the identification of D<sub>2</sub>like-selective ligands independently of chemical scaffolds. This could be especially important in diseases of the CNS, where D<sub>1</sub>R activation has been associated with induction of seizures. In addition, the D<sub>3</sub>R is a fast emerging molecular target of interest in treating PD. Thus, the accurate prediction of D<sub>2</sub>like-selectivity could act as an important starting point in developing truly D<sub>3</sub>R-selective compounds and also providing pharmacological tools to aid in the understanding of D<sub>2</sub>like DR subtype selectivity.

## 5. Conclusions

In this study, ten compounds were investigated for their DR subtype selectivity. A combined in silico/in vitro approach was developed to correlate the positioning within the receptor binding pocket with the biological activity. With the workflow, we observed a correlation between the distance of the ligand to the conserved glycine residue within the secondary binding pocket and the DR subtype selectivity. Most prominently, the workflow was able to identify D<sub>2</sub>like-selectivity but could not explain D<sub>2</sub>R/D<sub>3</sub>R selectivity observed in vitro. The most selective compound, **10**, was characterized by a low nano-molar activity at D<sub>3</sub>R (K<sub>i</sub> = 2.3 nM) showing a distinct selectivity over D<sub>1</sub>R and D<sub>2</sub>R with fold-differences of 1031.4 and 263.7, respectively. This study provides a valuable tool in further understanding DR subtype selectivity mechanisms, thus aiding the development of more selective DR ligands.

**Supplementary Materials:** The following supporting information can be downloaded at: <https://www.mdpi.com/article/10.3390/biomedicines11051468/s1>, Figure S1: Summary of the MDS approach for the modification of the D<sub>2</sub>R structure; Figures S2–S10: Summary of the in vitro screening results of all investigated compounds; Figure S11: Overview of the in vitro determined binding affinities of selected compounds (**1** and **3–9**); Figures S12–S17: Detailed insights into the docking poses and binding pockets of selected compounds (**3**, **5**, **6**, **7**, **8** and **9**); Table S1: Dataset of D<sub>1</sub>R-selective compounds (ChEMBL); Table S2: Dataset of D<sub>2</sub>R-selective compounds (ChEMBL); Table S3: Dataset of D<sub>2</sub>like-selective compounds (ChEMBL); Table S4: Dataset of D<sub>3</sub>R-selective compounds (ChEMBL); Table S5: Summary of the Minimization Process for the D<sub>2</sub>R structure; Table S6: Detailed overview of the settings used during the Minimization Process of the D<sub>2</sub>R structure; Table S7: Summary of the Standard Dynamics Cascade Process for the D<sub>2</sub>R structure; Table S8: Detailed overview of the settings used during the Standard Dynamics Cascade Process of the D<sub>2</sub>R structure; Table S9: Overview of 2D structures and NDF values; Table S10: Validation of in silico approach using ChEMBL; Table S11: Summary of the retrospective analysis of investigated compounds.

**Author Contributions:** Conceptualization. D.S.; methodology. L.Z.; software—commercially and publicly available software was used; validation. D.S., L.Z. and V.T.; investigation. A.B. and L.Z.; data curation. A.B. and L.Z.; writing—original draft preparation. L.Z.; writing—review and editing. D.S., L.Z. and V.T.; visualization. L.Z.; supervision. D.S. and V.T.; project administration. D.S. All authors have read and agreed to the published version of the manuscript.

**Funding:** V.T. is funded by the Austrian Science Fund (FWF) project T942. L.Z. is funded by PMU-RIF, 2022-PRE-005-Zell.

**Institutional Review Board Statement:** Not applicable.

**Informed Consent Statement:** Not applicable.



**Data Availability Statement:** The data presented in this study are available in the Supplementary Material. If further data are required, they are available from the corresponding author upon request.

**Conflicts of Interest:** The authors declare no conflict of interest.

## References

1. Hauser, A.S.; Attwood, M.M.; Rask-Andersen, M.; Schioth, H.B.; Gloriam, D.E. Trends in GPCR drug discovery: New agents, targets and indications. *Nat. Rev. Drug Discov.* **2017**, *16*, 829–842. [\[CrossRef\]](#)
2. Hauser, A.S.; Chavali, S.; Masuho, I.; Jahn, L.J.; Martemyanov, K.A.; Gloriam, D.E.; Babu, M.M. Pharmacogenomics of GPCR Drug Targets. *Cell* **2018**, *172*, 41–54.e19. [\[CrossRef\]](#) [\[PubMed\]](#)
3. Martel, J.C.; Gatti McArthur, S. Dopamine Receptor Subtypes, Physiology and Pharmacology: New Ligands and Concepts in Schizophrenia. *Front. Pharmacol.* **2020**, *11*, 11–17. [\[CrossRef\]](#) [\[PubMed\]](#)
4. Stocchi, F.; Torti, M.; Fossati, C. Advances in dopamine receptor agonists for the treatment of Parkinson's disease. *Expert Opin. Pharmacother.* **2016**, *17*, 1889–1902. [\[CrossRef\]](#) [\[PubMed\]](#)
5. Ashok, A.H.; Marques, T.R.; Jauhar, S.; Nour, M.M.; Goodwin, G.M.; Young, A.H.; Howes, O.D. The dopamine hypothesis of bipolar affective disorder: The state of the art and implications for treatment. *Mol. Psychiatry* **2017**, *22*, 666–679. [\[CrossRef\]](#)
6. Beaulieu, J.M.; Gainetdinov, R.R. The physiology, signaling, and pharmacology of dopamine receptors. *Pharmacol. Rev.* **2011**, *63*, 182–217. [\[CrossRef\]](#)
7. Kiss, B.; Laszlovsky, I.; Kramos, B.; Visegrady, A.; Levay, G.; Lendvai, B.; Roman, V. Neuronal Dopamine D3 Receptors: Translational Implications for Preclinical Research and CNS Disorders. *Biomolecules* **2021**, *11*, 104. [\[CrossRef\]](#)
8. Prieto, G.A. Abnormalities of Dopamine D(3) Receptor Signaling in the Diseased Brain. *J. Central Nerv. Syst. Dis.* **2017**, *9*, 1–8. [\[CrossRef\]](#)
9. Wang, Q.; Mach, R.H.; Luedtke, R.R.; Reichert, D.E. Subtype selectivity of dopamine receptor ligands: Insights from structure and ligand-based methods. *J. Chem. Inf. Model.* **2010**, *50*, 1970–1985. [\[CrossRef\]](#)
10. Murer, M.G.; Moratalla, R. Striatal Signaling in L-DOPA-Induced Dyskinesia: Common Mechanisms with Drug Abuse and Long Term Memory Involving D1 Dopamine Receptor Stimulation. *Front. Neuroanat.* **2011**, *5*, 51. [\[CrossRef\]](#)
11. Berman, B.D. Neuroleptic malignant syndrome: A review for neurohospitalists. *Neurohospitalist* **2011**, *1*, 41–47. [\[CrossRef\]](#) [\[PubMed\]](#)
12. Sykes, D.A.; Moore, H.; Stott, L.; Holliday, N.; Javitch, J.A.; Lane, J.R.; Charlton, S.J. Extrapyramidal side effects of antipsychotics are linked to their association kinetics at dopamine D(2) receptors. *Nat. Commun.* **2017**, *8*, 763. [\[CrossRef\]](#) [\[PubMed\]](#)
13. Lao, C.L.; Kuo, Y.H.; Hsieh, Y.T.; Chen, J.C. Intranasal and subcutaneous administration of dopamine D3 receptor agonists functionally restores nigrostriatal dopamine in MPTP-treated mice. *Neurotox. Res.* **2013**, *24*, 523–531. [\[CrossRef\]](#) [\[PubMed\]](#)
14. Li, C.; Biswas, S.; Li, X.; Dutta, A.K.; Le, W. Novel D3 dopamine receptor-preferring agonist D-264: Evidence of neuroprotective property in Parkinson's disease animal models induced by 1-methyl-4-phenyl-1,2,3,6-tetrahydropyridine and lactacystin. *J. Neurosci. Res.* **2010**, *88*, 2513–2523. [\[CrossRef\]](#)
15. Antonini, A.; Barone, P.; Ceravolo, R.; Fabbrini, G.; Tinazzi, M.; Abbruzzese, G. Role of pramipexole in the management of Parkinson's disease. *CNS Drugs* **2010**, *24*, 829–841. [\[CrossRef\]](#)
16. Carnicella, S.; Drui, G.; Boulet, S.; Carcenac, C.; Favier, M.; Duran, T.; Savasta, M. Implication of dopamine D3 receptor activation in the reversion of Parkinson's disease-related motivational deficits. *Transl. Psychiatry* **2014**, *4*, e401. [\[CrossRef\]](#)
17. Millan, M.J.; Gobert, A.; Newman-Tancredi, A.; Lejeune, F.; Cussac, D.; Rivet, J.M.; Audinot, V.; Dubuffet, T.; Lavielle, G. S33084, a novel, potent, selective, and competitive antagonist at dopamine D(3)-receptors: I. Receptorial, electrophysiological and neurochemical profile compared with GR218,231 and L741,626. *J. Pharmacol. Exp. Ther.* **2000**, *293*, 1048–1062.
18. Meltzer, H.Y. Cognitive factors in schizophrenia: Causes, impact, and treatment. *CNS Spectr.* **2004**, *9*, 15–24. [\[CrossRef\]](#)
19. Jones-Tabah, J.; Mohammad, H.; Paulus, E.G.; Clarke, P.B.S.; Herbert, T.E. The Signaling and Pharmacology of the Dopamine D1 Receptor. *Front. Cell. Neurosci.* **2021**, *15*, 806618. [\[CrossRef\]](#)
20. Felsing, D.E.; Jain, M.K.; Allen, J.A. Advances in Dopamine D1 Receptor Ligands for Neurotherapeutics. *Curr. Top. Med. Chem.* **2019**, *19*, 1365–1380. [\[CrossRef\]](#)
21. Girgis, R.R.; van Snellenberg, J.X.; Glass, A.; Kegeles, L.S.; Thompson, J.L.; Wall, M.; Cho, R.Y.; Carter, C.S.; Slifstein, M.; Abi-Dargham, A.; et al. A proof-of-concept, randomized controlled trial of DAR-0100A, a dopamine-1 receptor agonist, for cognitive enhancement in schizophrenia. *J. Psychopharmacol.* **2016**, *30*, 428–435. [\[CrossRef\]](#) [\[PubMed\]](#)
22. Rosell, D.R.; Zaluda, L.C.; McClure, M.M.; Strike, K.S.; Barch, D.M.; Harvey, P.D.; Girgis, R.R.; Hazlett, E.A.; Mailmann, R.B.; Abi-Dargham, A.; et al. Effects of the D1 dopamine receptor agonist dihydrexidine (DAR-0100A) on working memory in schizotypal personality disorder. *Neuropsychopharmacology* **2015**, *40*, 446–453. [\[CrossRef\]](#)
23. Abi-Dargham, A.; Javitch, J.A.; Slifstein, M.; Anticevic, A.; Calkins, M.E.; Cho, Y.T.; Fonteneau, C.; Gil, R.; Girgis, R.; Gur, R.E.; et al. Dopamine D1R Receptor Stimulation as a Mechanistic Pro-cognitive Target for Schizophrenia. *Schizophr. Bull.* **2022**, *48*, 199–210. [\[CrossRef\]](#) [\[PubMed\]](#)
24. O'Sullivan, G.J.; Dunleavy, M.; Hakansson, K.; Clementi, M.; Kinsella, A.; Croke, D.T.; Drago, J.; Fienberg, A.A.; Greengard, P.; Sibley, D.R.; et al. Dopamine D1 vs D5 receptor-dependent induction of seizures in relation to DARPP-32, ERK1/2 and GluR1-AMPA signalling. *Neuropharmacology* **2008**, *54*, 1051–1061. [\[CrossRef\]](#) [\[PubMed\]](#)

25. Arnsten, A.F.; Girgis, R.R.; Gray, D.L.; Mailman, R.B. Novel Dopamine Therapeutics for Cognitive Deficits in Schizophrenia. *Biol. Psychiatry* **2017**, *81*, 67–77. [[CrossRef](#)] [[PubMed](#)]
26. Kozak, R.; Kiss, T.; Dlugolenski, K.; Johnson, D.E.; Gorczyca, R.R.; Kuszpit, K.; Harvey, B.D.; Stolyar, P.; Sukoff Rizzo, S.J.; Hoffmann, W.E.; et al. Characterization of PF-6142, a Novel, Non-Catecholamine Dopamine Receptor D1 Agonist, in Murine and Nonhuman Primate Models of Dopaminergic Activation. *Front. Pharmacol.* **2020**, *11*, 1005. [[CrossRef](#)]
27. Basith, S.; Cui, M.; Macalino, S.J.Y.; Park, J.; Clavio, N.A.B.; Kang, S.; Choi, S. Exploring G Protein-Coupled Receptors (GPCRs) Ligand Space via Cheminformatics Approaches: Impact on Rational Drug Design. *Front. Pharmacol.* **2018**, *9*, 128. [[CrossRef](#)]
28. Salman, M.M.; Al-Obaidi, Z.; Kitchen, P.; Loreto, A.; Bill, R.M.; Wade-Martins, R. Advances in Applying Computer-Aided Drug Design for Neurodegenerative Diseases. *Int. J. Mol. Sci.* **2021**, *22*, 4688. [[CrossRef](#)]
29. Lian, P.; Xu, L.; Geng, C.; Qian, Y.; Li, W.; Zhen, X.; Fu, W. A computational perspective on drug discovery and signal transduction mechanism of dopamine and serotonin receptors in the treatment of schizophrenia. *Curr. Pharm. Biotechnol.* **2014**, *15*, 916–926. [[CrossRef](#)]
30. Nikolic, K.; Mavridis, L.; Djikic, T.; Vucicevic, J.; Agbaba, D.; Yelekci, K.; Mitchell, J.B. Drug Design for CNS Diseases: Polypharmacological Profiling of Compounds Using Cheminformatic, 3D-QSAR and Virtual Screening Methodologies. *Front. Neurosci.* **2016**, *10*, 265. [[CrossRef](#)]
31. Bueschbell, B.; Barreto, C.A.V.; Preto, A.J.; Schiedel, A.C.; Moreira, I.S. A Complete Assessment of Dopamine Receptor- Ligand Interactions through Computational Methods. *Molecules* **2019**, *24*, 1196. [[CrossRef](#)] [[PubMed](#)]
32. Floresca, C.Z.; Schetz, J.A. Dopamine receptor microdomains involved in molecular recognition and the regulation of drug affinity and function. *J. Recept. Signal Transduct. Res.* **2004**, *24*, 207–239. [[CrossRef](#)] [[PubMed](#)]
33. Vass, M.; Podlewska, S.; de Esch, I.J.P.; Bojarski, A.J.; Leurs, R.; Kooistra, A.J.; de Graaf, C. Aminergic GPCR-Ligand Interactions: A Chemical and Structural Map of Receptor Mutation Data. *J. Med. Chem.* **2019**, *62*, 3784–3839. [[CrossRef](#)] [[PubMed](#)]
34. Zhuang, Y.; Xu, P.; Mao, C.; Wang, L.; Krumm, B.; Zhou, X.E.; Huang, S.; Liu, H.; Cheng, X.; Huang, X.P.; et al. Structural insights into the human D1 and D2 dopamine receptor signaling complexes. *Cell* **2021**, *184*, 931–942.e18. [[CrossRef](#)] [[PubMed](#)]
35. Newman, A.H.; Beuming, T.; Banala, A.K.; Donthamsetti, P.; Pongetti, K.; LaBounty, A.; Levy, B.; Cao, J.; Michino, M.; Luedtke, R.R.; et al. Molecular determinants of selectivity and efficacy at the dopamine D3 receptor. *J. Med. Chem.* **2012**, *55*, 6689–6699. [[CrossRef](#)]
36. Michino, M.; Donthamsetti, P.; Beuming, T.; Banala, A.; Duan, L.; Roux, T.; Han, Y.; Trinquet, E.; Newman, A.H.; Javitch, J.A.; et al. A single glycine in extracellular loop 1 is the critical determinant for pharmacological specificity of dopamine D2 and D3 receptors. *Mol. Pharmacol.* **2013**, *84*, 854–864. [[CrossRef](#)]
37. Robinson, S.W.; Jarvie, K.R.; Caron, M.G. High affinity agonist binding to the dopamine D3 receptor: Chimeric receptors delineate a role for intracellular domains. *Mol. Pharmacol.* **1994**, *46*, 352–356.
38. Ishiki, H.M.; Filho, J.M.B.; da Silva, M.S.; Scotti, M.T.; Scotti, L. Computer-aided Drug Design Applied to Parkinson Targets. *Curr. Neuropharmacol.* **2018**, *16*, 865–880. [[CrossRef](#)]
39. Elek, M.; Djokovic, N.; Frank, A.; Oljatic, S.; Zivkovic, A.; Nikolic, K.; Stark, H. Synthesis, in silico, and in vitro studies of novel dopamine D(2) and D(3) receptor ligands. *Arch. Pharm.* **2021**, *354*, e2000486. [[CrossRef](#)]
40. Degorce, F.; Card, A.; Soh, S.; Trinquet, E.; Knapik, G.P.; Xie, B. HTRF: A technology tailored for drug discovery—A review of the theoretical aspects and recent applications. *Curr. Chem. Genom.* **2009**, *3*, 22–32. [[CrossRef](#)]
41. Yasi, E.A.; Kruyer, N.S.; Peralta-Yahya, P. Advances in G protein-coupled receptor high-throughput screening. *Curr. Opin. Biotechnol.* **2020**, *64*, 210–217. [[CrossRef](#)] [[PubMed](#)]
42. Zell, L.; Lainer, C.; Kollar, J.; Temml, V.; Schuster, D. Identification of Novel Dopamine D(2) Receptor Ligands-A Combined In Silico/In Vitro Approach. *Molecules* **2022**, *27*, 4435. [[CrossRef](#)] [[PubMed](#)]
43. Glen, R.C.; Bender, A.; Arnby, C.H.; Carlsson, L.; Boyer, S.; Smith, J. Circular fingerprints: Flexible molecular descriptors with applications from physical chemistry to ADME. *IDrugs* **2006**, *9*, 199–204.
44. Rogers, D.; Hahn, M. Extended-connectivity fingerprints. *J. Chem. Inf. Model.* **2010**, *50*, 742–754. [[CrossRef](#)]
45. Tanimoto, T.T. *An Elementary Mathematical Theory of Classification and Prediction*; International Business Machines Corporation: Armonk, NY, USA, 1958.
46. el Ahmad, Y.; Laurent, E.; Maillet, P.; Talab, A.; Teste, J.F.; Dokhan, R.; Tran, G.; Ollivier, R. New benzocycloalkylpiperazines, potent and selective 5-HT1A receptor ligands. *J. Med. Chem.* **1997**, *40*, 952–960. [[CrossRef](#)]
47. Hubner, H.; Kraxner, J.; Gmeiner, P. Cyanoindole derivatives as highly selective dopamine D(4) receptor partial agonists: Solid-phase synthesis, binding assays, and functional experiments. *J. Med. Chem.* **2000**, *43*, 4563–4569. [[CrossRef](#)]
48. Einsiedel, J.; Hubner, H.; Gmeiner, P. Benzamide bioisosteres incorporating dihydroheteroazole substructures: EPC synthesis and SAR leading to a selective dopamine D4 receptor partial agonist (FAUC 179). *Bioorg. Med. Chem. Lett.* **2001**, *11*, 2533–2536. [[CrossRef](#)]
49. Lober, S.; Aboul-Fadl, T.; Hubner, H.; Gmeiner, P. Di- and trisubstituted pyrazolo[1,5-a]pyridine derivatives: Synthesis, dopamine receptor binding and ligand efficacy. *Bioorg. Med. Chem. Lett.* **2002**, *12*, 633–636. [[CrossRef](#)]
50. Wittig, T.W.; Decker, M.; Lehmann, J. Dopamine/serotonin receptor ligands. 9. Oxygen-containing midsized heterocyclic ring systems and nonrigidized analogues. A step toward dopamine D5 receptor selectivity. *J. Med. Chem.* **2004**, *47*, 4155–4158. [[CrossRef](#)]

51. Seong, C.M.; Park, W.K.; Park, C.M.; Kong, J.Y.; Park, N.S. Discovery of 3-aryl-3-methyl-1H-quinoline-2,4-diones as a new class of selective 5-HT<sub>6</sub> receptor antagonists. *Bioorg. Med. Chem. Lett.* **2008**, *18*, 738–743. [[CrossRef](#)]
52. Enzensperger, C.; Muller, F.K.; Schmalwasser, B.; Wiecha, P.; Traber, H.; Lehmann, J. Dopamine/serotonin receptor ligands. 16.(1) Expanding dibenz[d,g]azecines to 11- and 12-membered homologues. Interaction with dopamine D(1)-D(5) receptors. *J. Med. Chem.* **2007**, *50*, 4528–4533. [[CrossRef](#)] [[PubMed](#)]
53. Linz, S.; Muller, J.; Hubner, H.; Gmeiner, P.; Troschutz, R. Design, synthesis and dopamine D<sub>4</sub> receptor binding activities of new N-heteroaromatic 5/6-ring Mannich bases. *Bioorg. Med. Chem.* **2009**, *17*, 4448–4458. [[CrossRef](#)] [[PubMed](#)]
54. Banister, S.D.; Moussa, I.A.; Jorgensen, W.T.; Chua, S.W.; Kassiou, M. Molecular hybridization of 4-azahexacyclo[5.4.1.0(2,6).0(3,10).0(5,9).0(8,11)]dodecane-3-ol with sigma (sigma) receptor ligands modulates off-target activity and subtype selectivity. *Bioorg. Med. Chem. Lett.* **2011**, *21*, 3622–3626. [[CrossRef](#)] [[PubMed](#)]
55. Robaa, D.; Enzensperger, C.; Eldin Abulazm, S.; Hefnawy, M.M.; El-Subbagh, H.I.; Wani, T.A.; Lehmann, J. Chiral indolo[3,2-f][3]benzazecine-type dopamine receptor antagonists: Synthesis and activity of racemic and enantiopure derivatives. *J. Med. Chem.* **2011**, *54*, 7422–7426. [[CrossRef](#)]
56. Sampson, D.; Zhu, X.Y.; Eyunni, S.V.; Etukala, J.R.; Ofori, E.; Bricker, B.; Lamango, N.S.; Setola, V.; Roth, B.L.; Ablordeppey, S.Y. Identification of a new selective dopamine D<sub>4</sub> receptor ligand. *Bioorg. Med. Chem.* **2014**, *22*, 3105–3114. [[CrossRef](#)]
57. Zhang, J.; Huang, J.; Song, Z.; Guo, L.; Cai, W.; Wang, Y.; Zhen, X.; Zhang, A. Structural manipulation on the catecholic fragment of dopamine D(1) receptor agonist 1-phenyl-N-methyl-benzazepines. *Eur. J. Med. Chem.* **2014**, *85*, 16–26. [[CrossRef](#)]
58. Madapa, S.; Harding, W.W. Semisynthetic Studies on and Biological Evaluation of N-Methylaurotetanine Analogues as Ligands for 5-HT Receptors. *J. Nat. Prod.* **2015**, *78*, 722–729. [[CrossRef](#)]
59. Lee, D.Y.W.; Liu, J.; Zhang, S.; Huang, P.; Liu-Chen, L.Y. Asymmetric total synthesis of tetrahydroprotoberberine derivatives and evaluation of their binding affinities at dopamine receptors. *Bioorg. Med. Chem. Lett.* **2017**, *27*, 1437–1440. [[CrossRef](#)]
60. Martini, M.L.; Liu, J.; Ray, C.; Yu, X.; Huang, X.P.; Urs, A.; Urs, N.; McCorvy, J.D.; Caron, M.G.; Roth, B.L.; et al. Defining Structure-Functional Selectivity Relationships (SFSR) for a Class of Non-Catechol Dopamine D(1) Receptor Agonists. *J. Med. Chem.* **2019**, *62*, 3753–3772. [[CrossRef](#)]
61. Heier, R.F.; Dolak, L.A.; Duncan, J.N.; Hyslop, D.K.; Lipton, M.F.; Martin, I.J.; Mauragis, M.A.; Piercey, M.F.; Nichols, N.F.; Schreur, P.J.; et al. Synthesis and biological activities of (R)-5,6-dihydro-N,N-dimethyl-4H-imidazo[4,5,1-ij]quinolin-5-amine and its metabolites. *J. Med. Chem.* **1997**, *40*, 639–646. [[CrossRef](#)]
62. Thomas, C.; Hubner, H.; Gmeiner, P. Enantio- and diastereocontrolled dopamine D<sub>1</sub>, D<sub>2</sub>, D<sub>3</sub> and D<sub>4</sub> receptor binding of N-(3-pyrrolidinylmethyl)benzamides synthesized from aspartic acid. *Bioorg. Med. Chem. Lett.* **1999**, *9*, 841–846. [[CrossRef](#)] [[PubMed](#)]
63. Einsiedel, J.; Thomas, C.; Hubner, H.; Gmeiner, P. Phenylloxazoles and phenylthiazoles as benzamide bioisosteres: Synthesis and dopamine receptor binding profiles. *Bioorg. Med. Chem. Lett.* **2000**, *10*, 2041–2044. [[CrossRef](#)] [[PubMed](#)]
64. Lehmann, T.; Hubner, H.; Gmeiner, P. Dopaminergic 7-aminotetrahydroindolizines: Ex-chiral pool synthesis and preferential D<sub>3</sub> receptor binding. *Bioorg. Med. Chem. Lett.* **2001**, *11*, 2863–2866. [[CrossRef](#)] [[PubMed](#)]
65. Einsiedel, J.; Weber, K.; Thomas, C.; Lehmann, T.; Hubner, H.; Gmeiner, P. Stereocontrolled dopamine receptor binding and subtype selectivity of clebopride analogues synthesized from aspartic acid. *Bioorg. Med. Chem. Lett.* **2003**, *13*, 3293–3296. [[CrossRef](#)]
66. Enguehard-Gueiffier, C.; Hubner, H.; el Hakmaoui, A.; Allouchi, H.; Gmeiner, P.; Argiolas, A.; Melis, M.R.; Gueiffier, A. 2-[(4-phenylpiperazin-1-yl)methyl]imidazo(di)azines as selective D<sub>4</sub>-ligands. Induction of penile erection by 2-[4-(2-methoxyphenyl)piperazin-1-ylmethyl]imidazo[1,2-a]pyridine (PIP3EA), a potent and selective D<sub>4</sub> partial agonist. *J. Med. Chem.* **2006**, *49*, 3938–3947. [[CrossRef](#)]
67. Tietze, R.; Lober, S.; Hubner, H.; Gmeiner, P.; Kuwert, T.; Prante, O. Discovery of a dopamine D<sub>4</sub> selective PET ligand candidate taking advantage of a click chemistry based REM linker. *Bioorg. Med. Chem. Lett.* **2008**, *18*, 983–988. [[CrossRef](#)]
68. Balle, T.; Perregaard, J.; Ramirez, M.T.; Larsen, A.K.; Soby, K.K.; Liljefors, T.; Andersen, K. Synthesis and structure-affinity relationship investigations of 5-heteroaryl-substituted analogues of the antipsychotic sertindole. A new class of highly selective alpha(1) adrenoceptor antagonists. *J. Med. Chem.* **2003**, *46*, 265–283. [[CrossRef](#)]
69. Sromek, A.W.; Si, Y.G.; Zhang, T.; George, S.R.; Seeman, P.; Neumeyer, J.L. Synthesis and Evaluation of Fluorinated Aporphines: Potential Positron Emission Tomography Ligands for D<sub>2</sub> Receptors. *ACS Med. Chem. Lett.* **2011**, *2*, 189–194. [[CrossRef](#)]
70. Banerjee, A.; Maschauer, S.; Hubner, H.; Gmeiner, P.; Prante, O. Click chemistry based synthesis of dopamine D<sub>4</sub> selective receptor ligands for the selection of potential PET tracers. *Bioorg. Med. Chem. Lett.* **2013**, *23*, 6079–6082. [[CrossRef](#)]
71. Salama, I.; Lober, S.; Hubner, H.; Gmeiner, P. Synthesis and binding profile of haloperidol-based bivalent ligands targeting dopamine D(2)-like receptors. *Bioorg. Med. Chem. Lett.* **2014**, *24*, 3753–3756. [[CrossRef](#)]
72. Lindsley, C.W.; Hopkins, C.R. Return of D(4) Dopamine Receptor Antagonists in Drug Discovery. *J. Med. Chem.* **2017**, *60*, 7233–7243. [[CrossRef](#)] [[PubMed](#)]
73. Glase, S.A.; Akunne, H.C.; Heffner, T.G.; Jaen, J.C.; MacKenzie, R.G.; Meltzer, L.T.; Pugsley, T.A.; Smith, S.J.; Wise, L.D. Aryl 1-but-3-ynyl-4-phenyl-1,2,3,6-tetrahydropyridines as potential antipsychotic agents: Synthesis and structure-activity relationships. *J. Med. Chem.* **1996**, *39*, 3179–3187. [[CrossRef](#)]
74. Yuan, J.; Chen, X.; Brodbeck, R.; Primus, R.; Braun, J.; Wasley, J.W.; Thurkauf, A. NGB 2904 and NGB 2849: Two highly selective dopamine D<sub>3</sub> receptor antagonists. *Bioorg. Med. Chem. Lett.* **1998**, *8*, 2715–2718. [[CrossRef](#)] [[PubMed](#)]



75. Birch, A.M.; Bradley, P.A.; Gill, J.C.; Kerrigan, F.; Needham, P.L. N-Substituted (2,3-dihydro-1,4-benzodioxin-2-yl)methylamine derivatives as D(2) antagonists/5-HT(1A) partial agonists with potential as atypical antipsychotic agents. *J. Med. Chem.* **1999**, *42*, 3342–3355. [[CrossRef](#)]
76. Paul, N.M.; Taylor, M.; Kumar, R.; Deschamps, J.R.; Luedtke, R.R.; Newman, A.H. Structure-activity relationships for a novel series of dopamine D2-like receptor ligands based on N-substituted 3-aryl-8-azabicyclo[3.2.1]octan-3-ol. *J. Med. Chem.* **2008**, *51*, 6095–6109. [[CrossRef](#)] [[PubMed](#)]
77. Kumar, J.S.; Majo, V.J.; Hsiung, S.C.; Millak, M.S.; Liu, K.P.; Tamir, H.; Prabhakaran, J.; Simpson, N.R.; van Heertum, R.L.; Mann, J.J.; et al. Synthesis and in vivo validation of [O-methyl-11C]2-4-[4-(7-methoxynaphthalen-1-yl)piperazin-1-yl]butyl-4-methyl-2H-[1,2,4]triazine-3,5-dione: A novel 5-HT1A receptor agonist positron emission tomography ligand. *J. Med. Chem.* **2006**, *49*, 125–134. [[CrossRef](#)]
78. Schlotter, K.; Boeckler, F.; Huber, H.; Gmeiner, P. Fancy bioisosteres: Novel paracyclophane derivatives as super-affinity dopamine D3 receptor antagonists. *J. Med. Chem.* **2006**, *49*, 3628–3635. [[CrossRef](#)]
79. Newman, A.H.; Grundt, P.; Cyriac, G.; Deschamps, J.R.; Taylor, M.; Kumar, R.; Ho, D.; Luedtke, R.R. N-(4-(4-(2,3-dichloro- or 2-methoxyphenyl)piperazin-1-yl)butyl)heterobiarylcarboxamides with functionalized linking chains as high affinity and enantioselective D3 receptor antagonists. *J. Med. Chem.* **2009**, *52*, 2559–2570. [[CrossRef](#)]
80. Ortega, R.; Ravina, E.; Masaguer, C.F.; Areias, F.; Brea, J.; Loza, M.I.; Lopez, L.; Selent, J.; Pastor, M.; Sanz, F. Synthesis, binding affinity and SAR of new benzolactam derivatives as dopamine D3 receptor ligands. *Bioorg. Med. Chem. Lett.* **2009**, *19*, 1773–1778. [[CrossRef](#)]
81. Skultety, M.; Hubner, H.; Lober, S.; Gmeiner, P. Bioisosteric replacement leading to biologically active [2,2]paracyclophanes with altered binding profiles for aminergic G-protein-coupled receptors. *J. Med. Chem.* **2010**, *53*, 7219–7228. [[CrossRef](#)]
82. Hofling, S.B.; Maschauer, S.; Hubner, H.; Gmeiner, P.; Wester, H.J.; Prante, O.; Heinrich, M.R. Synthesis, biological evaluation and radiolabelling by 18F-fluoroarylation of a dopamine D3-selective ligand as prospective imaging probe for PET. *Bioorg. Med. Chem. Lett.* **2010**, *20*, 6933–6937. [[CrossRef](#)] [[PubMed](#)]
83. Ye, N.; Wu, Q.; Zhu, L.; Zheng, L.; Gao, B.; Zhen, X.; Zhang, A. Further SAR study on 11-O-substituted aporphine analogues: Identification of highly potent dopamine D3 receptor ligands. *Bioorg. Med. Chem.* **2011**, *19*, 1999–2008. [[CrossRef](#)] [[PubMed](#)]
84. Reinart-Okugbeni, R.; Ausmees, K.; Kriis, K.; Werner, F.; Rinken, A.; Kanger, T. Chemoenzymatic synthesis and evaluation of 3-azabicyclo[3.2.0]heptane derivatives as dopaminergic ligands. *Eur. J. Med. Chem.* **2012**, *55*, 255–261. [[CrossRef](#)] [[PubMed](#)]
85. Spetea, M.; Berzetei-Gurske, I.P.; Guerrieri, E.; Schmidhammer, H. Discovery and pharmacological evaluation of a diphenethylamine derivative (HS665), a highly potent and selective kappa opioid receptor agonist. *J. Med. Chem.* **2012**, *55*, 10302–10306. [[CrossRef](#)]
86. Majo, V.J.; Milak, M.S.; Prabhakaran, J.; Mali, P.; Savenkova, L.; Simpson, N.R.; Mann, J.J.; Parsey, R.V.; Kumar, J.S. Synthesis and in vivo evaluation of [(18F)2-(4-(4-(2-(2-fluoroethoxy)phenyl)piperazin-1-yl)butyl)-4-methyl-1,2,4-triazine-3,5(2H,4H)-dione] ([18F]FECUMI-101) as an imaging probe for 5-HT1A receptor agonist in nonhuman primates. *Bioorg. Med. Chem.* **2013**, *21*, 5598–5604. [[CrossRef](#)]
87. Abdelfattah, M.A.; Lehmann, J.; Abadi, A.H. Discovery of highly potent and selective D4 ligands by interactive SAR study. *Bioorg. Med. Chem. Lett.* **2013**, *23*, 5077–5081. [[CrossRef](#)]
88. Insua, I.; Alvarado, M.; Masaguer, C.F.; Iglesias, A.; Brea, J.; Loza, M.I.; Carro, L. Synthesis and binding affinity of new 1,4-disubstituted triazoles as potential dopamine D(3) receptor ligands. *Bioorg. Med. Chem. Lett.* **2013**, *23*, 5586–5591. [[CrossRef](#)]
89. van Wieringen, J.P.; Shalgunov, V.; Janssen, H.M.; Fransen, P.M.; Janssen, A.G.; Michel, M.C.; Booij, J.; Elsinga, P.H. Synthesis and characterization of a novel series of agonist compounds as potential radiopharmaceuticals for imaging dopamine D(2)/(3) receptors in their high-affinity state. *J. Med. Chem.* **2014**, *57*, 391–410. [[CrossRef](#)]
90. Moller, D.; Kling, R.C.; Skultety, M.; Leuner, K.; Hubner, H.; Gmeiner, P. Functionally selective dopamine D(2), D(3) receptor partial agonists. *J. Med. Chem.* **2014**, *57*, 4861–4875. [[CrossRef](#)]
91. Sampson, D.; Bricker, B.; Zhu, X.Y.; Peprah, K.; Lamango, N.S.; Setola, V.; Roth, B.L.; Ablordeppey, S.Y. Further evaluation of the tropane analogs of haloperidol. *Bioorg. Med. Chem. Lett.* **2014**, *24*, 4294–4297. [[CrossRef](#)]
92. Weichert, D.; Banerjee, A.; Hiller, C.; Kling, R.C.; Hubner, H.; Gmeiner, P. Molecular determinants of biased agonism at the dopamine D(2) receptor. *J. Med. Chem.* **2015**, *58*, 2703–2717. [[CrossRef](#)] [[PubMed](#)]
93. Jorg, M.; Kaczor, A.A.; Mak, F.S.; Lee, K.C.K.; Poso, A.; Miller, N.D.; Scammells, P.J.; Capuano, B. Investigation of novel ropinirole analogues: Synthesis, pharmacological evaluation and computational analysis of dopamine D-2 receptor functionalized congeners and homobivalent ligands. *MedChemComm* **2014**, *5*, 891–898. [[CrossRef](#)]
94. Bartuschat, A.L.; Schellhorn, T.; Hubner, H.; Gmeiner, P.; Heinrich, M.R. Fluoro-substituted phenylazocarboxamides: Dopaminergic behavior and N-arylation properties for irreversible binding. *Bioorg. Med. Chem.* **2015**, *23*, 3938–3947. [[CrossRef](#)] [[PubMed](#)]
95. Moller, D.; Salama, I.; Kling, R.C.; Hubner, H.; Gmeiner, P. 1,4-Disubstituted aromatic piperazines with high 5-HT2A/D2 selectivity: Quantitative structure-selectivity investigations, docking, synthesis and biological evaluation. *Bioorg. Med. Chem.* **2015**, *23*, 6195–6209. [[CrossRef](#)] [[PubMed](#)]
96. Weichert, D.; Stanek, M.; Hubner, H.; Gmeiner, P. Structure-guided development of dual beta2 adrenergic/dopamine D2 receptor agonists. *Bioorg. Med. Chem.* **2016**, *24*, 2641–2653. [[CrossRef](#)]

97. Moller, D.; Banerjee, A.; Uzuneser, T.C.; Skultety, M.; Huth, T.; Plouffe, B.; Hubner, H.; Alzheimer, C.; Friedland, K.; Muller, C.P.; et al. Discovery of G Protein-Biased Dopaminergics with a Pyrazolo[1,5-a]pyridine Substructure. *J. Med. Chem.* **2017**, *60*, 2908–2929. [[CrossRef](#)]
98. Mannel, B.; Dengler, D.; Shonberg, J.; Hubner, H.; Moller, D.; Gmeiner, P. Hydroxy-Substituted Heteroaryl piperazines: Novel Scaffolds for beta-Arrestin-Biased D(2)R Agonists. *J. Med. Chem.* **2017**, *60*, 4693–4713. [[CrossRef](#)]
99. Mannel, B.; Hubner, H.; Moller, D.; Gmeiner, P. beta-Arrestin biased dopamine D2 receptor partial agonists: Synthesis and pharmacological evaluation. *Bioorg. Med. Chem.* **2017**, *25*, 5613–5628. [[CrossRef](#)]
100. Stossel, A.; Brox, R.; Purkayastha, N.; Hubner, H.; Hocke, C.; Prante, O.; Gmeiner, P. Development of molecular tools based on the dopamine D(3) receptor ligand FAUC 329 showing inhibiting effects on drug and food maintained behavior. *Bioorg. Med. Chem.* **2017**, *25*, 3491–3499. [[CrossRef](#)]
101. Omran, A.; Eslamimehr, S.; Crider, A.M.; Neumann, W.L. Synthesis of 3-(3-hydroxyphenyl)pyrrolidine dopamine D(3) receptor ligands with extended functionality for probing the secondary binding pocket. *Bioorg. Med. Chem. Lett.* **2018**, *28*, 1897–1902. [[CrossRef](#)]
102. Ashraf-Uz-Zaman, M.; Sajib, M.S.; Cucullo, L.; Mikelis, C.M.; German, N.A. Analogs of penfluridol as chemotherapeutic agents with reduced central nervous system activity. *Bioorg. Med. Chem. Lett.* **2018**, *28*, 3652–3657. [[CrossRef](#)] [[PubMed](#)]
103. Chen, P.J.; Taylor, M.; Griffin, S.A.; Amani, A.; Hayatshahi, H.; Korzekwa, K.; Ye, M.; Mach, R.H.; Liu, J.; Luedtke, R.R.; et al. Design, synthesis, and evaluation of N-(4-(4-phenyl piperazin-1-yl)butyl)-4-(thiophen-3-yl)benzamides as selective dopamine D(3) receptor ligands. *Bioorg. Med. Chem. Lett.* **2019**, *29*, 2690–2694. [[CrossRef](#)] [[PubMed](#)]
104. Tan, L.; Zhou, Q.; Yan, W.; Sun, J.; Kozikowski, A.P.; Zhao, S.; Huang, X.P.; Cheng, J. Design and Synthesis of Bitopic 2-Phenylcyclopropylmethylamine (PCPMA) Derivatives as Selective Dopamine D3 Receptor Ligands. *J. Med. Chem.* **2020**, *63*, 4579–4602. [[CrossRef](#)]
105. Moritz, A.E.; Free, R.B.; Weiner, W.S.; Akano, E.O.; Gandhi, D.; Abramyan, A.; Keck, T.M.; Ferrer, M.; Hu, X.; Southall, N.; et al. Discovery, Optimization, and Characterization of ML417: A Novel and Highly Selective D(3) Dopamine Receptor Agonist. *J. Med. Chem.* **2020**, *63*, 5526–5567. [[CrossRef](#)] [[PubMed](#)]
106. Battiti, F.O.; Newman, A.H.; Bonifazi, A. Exception That Proves the Rule: Investigation of Privileged Stereochemistry in Designing Dopamine D(3)R Bitopic Agonists. *ACS Med. Chem. Lett.* **2020**, *11*, 1956–1964. [[CrossRef](#)] [[PubMed](#)]
107. Bergauer, M.; Hubner, H.; Gmeiner, P. 2,4-Disubstituted pyrroles: Synthesis, traceless linking and pharmacological investigations leading to the dopamine D4 receptor partial agonist FAUC 356. *Bioorg. Med. Chem. Lett.* **2002**, *12*, 1937–1940. [[CrossRef](#)]
108. Bettinetti, L.; Schlotter, K.; Hubner, H.; Gmeiner, P. Interactive SAR studies: Rational discovery of super-potent and highly selective dopamine D3 receptor antagonists and partial agonists. *J. Med. Chem.* **2002**, *45*, 4594–4597. [[CrossRef](#)]
109. Hocke, C.; Prante, O.; Lober, S.; Hubner, H.; Gmeiner, P.; Kuwert, T. Synthesis and radioiodination of selective ligands for the dopamine D3 receptor subtype. *Bioorg. Med. Chem. Lett.* **2004**, *14*, 3963–3966. [[CrossRef](#)]
110. Rodriguez Loaiza, P.; Lober, S.; Hubner, H.; Gmeiner, P. Click chemistry based solid phase supported synthesis of dopaminergic phenylacetyles. *Bioorg. Med. Chem.* **2007**, *15*, 7248–7257. [[CrossRef](#)]
111. Butini, S.; Gemma, S.; Campiani, G.; Franceschini, S.; Trotta, F.; Borriello, M.; Ceres, N.; Ros, S.; Coccone, S.S.; Bernetti, M.; et al. Discovery of a new class of potential multifunctional atypical antipsychotic agents targeting dopamine D3 and serotonin 5-HT1A and 5-HT2A receptors: Design, synthesis, and effects on behavior. *J. Med. Chem.* **2009**, *52*, 151–169. [[CrossRef](#)]
112. Dorfler, M.; Tschammer, N.; Hamperl, K.; Hubner, H.; Gmeiner, P. Novel D3 selective dopaminergics incorporating enyne units as nonaromatic catechol bioisosteres: Synthesis, bioactivity, and mutagenesis studies. *J. Med. Chem.* **2008**, *51*, 6829–6838. [[CrossRef](#)] [[PubMed](#)]
113. von Coburg, Y.; Kottke, T.; Weizel, L.; Ligneau, X.; Stark, H. Potential utility of histamine H3 receptor antagonist pharmacophore in antipsychotics. *Bioorg. Med. Chem. Lett.* **2009**, *19*, 538–542. [[CrossRef](#)] [[PubMed](#)]
114. Tschammer, N.; Elsner, J.; Goetz, A.; Ehrlich, K.; Schuster, S.; Ruberg, M.; Kuhhorn, J.; Thompson, D.; Whistler, J.; Hubner, H.; et al. Highly potent 5-aminotetrahydropyrazolopyridines: Enantioselective dopamine D3 receptor binding, functional selectivity, and analysis of receptor-ligand interactions. *J. Med. Chem.* **2011**, *54*, 2477–2491. [[CrossRef](#)] [[PubMed](#)]
115. Berry, C.B.; Bubser, M.; Jones, C.K.; Hayes, J.P.; Wepy, J.A.; Locuson, C.W.; Daniels, J.S.; Lindsley, C.W.; Hopkins, C.R. Discovery and Characterization of ML398, a Potent and Selective Antagonist of the D4 Receptor with in Vivo Activity. *ACS Med. Chem. Lett.* **2014**, *5*, 1060–1064. [[CrossRef](#)] [[PubMed](#)]
116. Ponnala, S.; Kapadia, N.; Harding, W.W. Identification of tris-(phenylalkyl) amines as new selective h5-HT2B receptor antagonists. *MedChemComm* **2015**, *6*, 601–605. [[CrossRef](#)]
117. Gadhiya, S.; Cordone, P.; Pal, R.K.; Gallicchio, E.; Wickstrom, L.; Kurtzmann, T.; Ramsey, S.; Harding, W.W. New Dopamine D3-Selective Receptor Ligands Containing a 6-Methoxy-1,2,3,4-tetrahydroisoquinolin-7-ol Motif. *ACS Med. Chem. Lett.* **2018**, *9*, 990–995. [[CrossRef](#)]
118. Karki, A.; Namballa, H.K.; Alberts, I.; Harding, W.W. Structural manipulation of aporphines via C10 nitrogenation leads to the identification of new 5-HT(7A)R ligands. *Bioorg. Med. Chem.* **2020**, *28*, 115578. [[CrossRef](#)]
119. Hawkins, P.C.; Skillman, A.G.; Warren, G.L.; Ellingson, B.A.; Stahl, M.T. Conformer generation with OMEGA: Algorithm and validation using high quality structures from the Protein Databank and Cambridge Structural Database. *J. Chem. Inf. Model.* **2010**, *50*, 572–584. [[CrossRef](#)]



120. Jones, G.; Willett, P.; Glen, R.C.; Leach, A.R.; Taylor, R. Development and validation of a genetic algorithm for flexible docking. *J. Mol. Biol.* **1997**, *267*, 727–748. [[CrossRef](#)]
121. Xu, P.; Huang, S.; Mao, C.; Krumm, B.E.; Zhou, X.E.; Tan, Y.; Huang, X.P.; Liu, Y.; Shen, D.D.; Jiang, Y.; et al. Structures of the human dopamine D3 receptor-G(i) complexes. *Mol. Cell.* **2021**, *81*, 1147–1159.e4. [[CrossRef](#)]
122. Altschul, S.F.; Gish, W.; Miller, W.; Myers, E.W.; Lipman, D.J. Basic local alignment search tool. *J. Mol. Biol.* **1990**, *215*, 403–410. [[CrossRef](#)] [[PubMed](#)]
123. BIOVIA. *Dassault Systèmes, BIOVIA Discovery Studio, Release 2018*; Dassault Systems: San Diego, CA, USA, 2018.
124. Wolber, G.; Langer, T. LigandScout: 3-D pharmacophores derived from protein-bound ligands and their use as virtual screening filters. *J. Chem. Inf. Model.* **2005**, *45*, 160–169. [[CrossRef](#)] [[PubMed](#)]
125. Joobar, R.; Boksa, P. Clozapine: A distinct, poorly understood and under-used molecule. *J. Psychiatry Neurosci.* **2010**, *35*, 147–149. [[CrossRef](#)]
126. Garcia-Romero, E.M.; López-López, E.; Soriano-Correa, C.; Medina-Franco, J.L.; Barrientos-Salcedo, C. Polypharmacological drug design opportunities against Parkinson's disease. *F1000Research* **2022**, *11*, 1176. [[CrossRef](#)]
127. Perrone, R.; Berardi, F.; Colabufo, N.A.; Leopoldo, M.; Tortorella, V. A structure-affinity relationship study on derivatives of N-[2-[4-(4-Chlorophenyl)piperazin-1-yl]ethyl]-3-methoxybenzamide, a high-affinity and selective D(4) receptor ligand. *J. Med. Chem.* **2000**, *43*, 270–277. [[CrossRef](#)]
128. Smith, J.L.; Stein, D.A.; Shum, D.; Fischer, M.A.; Radu, C.; Bhinder, B.; Djballah, H.; Nelson, J.A.; Fruh, K.; Hirsch, A.J. Inhibition of dengue virus replication by a class of small-molecule compounds that antagonize dopamine receptor d4 and downstream mitogen-activated protein kinase signaling. *J. Virol.* **2014**, *88*, 5533–5542. [[CrossRef](#)]
129. Campiani, G.; Nacci, V.; Bechelli, S.; Ciani, S.M.; Garofalo, A.; Fiorini, I.; Wikstrom, H.; de Boer, P.; Liao, Y.; Tepper, P.G.; et al. New antipsychotic agents with serotonin and dopamine antagonist properties based on a pyrrolo[2,1-b][1,3]benzothiazepine structure. *J. Med. Chem.* **1998**, *41*, 3763–3772. [[CrossRef](#)]
130. Staron, J.; Kurczab, R.; Warszycki, D.; Satala, G.; Krawczyk, M.; Bugno, R.; Lenda, T.; Popik, P.; Hogendorf, A.S.; Hogendorf, A.; et al. Virtual screening-driven discovery of dual 5-HT(6)/5-HT(2A) receptor ligands with pro-cognitive properties. *Eur. J. Med. Chem.* **2020**, *185*, 111857. [[CrossRef](#)]
131. Peprah, K.; Zhu, X.Y.; Eyunni, S.V.; Setola, V.; Roth, B.L.; Ablordeppey, S.Y. Multi-receptor drug design: Haloperidol as a scaffold for the design and synthesis of atypical antipsychotic agents. *Bioorg. Med. Chem.* **2012**, *20*, 1291–1297. [[CrossRef](#)]
132. Schoemaker, H.; Claustre, Y.; Fage, D.; Rouquier, L.; Chergui, K.; Curet, O.; Oblin, A.; Gonon, F.; Carter, C.; Benavides, J.; et al. Neurochemical characteristics of amisulpride, an atypical dopamine D2/D3 receptor antagonist with both presynaptic and limbic selectivity. *J. Pharmacol. Exp. Ther.* **1997**, *280*, 83–97.
133. Daina, A.; Michielin, O.; Zoete, V. SwissTargetPrediction: Updated data and new features for efficient prediction of protein targets of small molecules. *Nucleic Acids Res.* **2019**, *47*, W357–W364. [[CrossRef](#)] [[PubMed](#)]
134. Bragina, M.E.; Daina, A.; Perez, M.A.S.; Michielin, O.; Zoete, V. The SwissSimilarity 2021 Web Tool: Novel Chemical Libraries and Additional Methods for an Enhanced Ligand-Based Virtual Screening Experience. *Int. J. Mol. Sci.* **2022**, *23*, 811. [[CrossRef](#)] [[PubMed](#)]
135. Zoete, V.; Daina, A.; Bovigny, C.; Michielin, O. SwissSimilarity: A Web Tool for Low to Ultra High Throughput Ligand-Based Virtual Screening. *J. Chem. Inf. Model.* **2016**, *56*, 1399–1404. [[CrossRef](#)] [[PubMed](#)]
136. Charifson, P.S.; Bowen, J.P.; Wyrick, S.D.; Hoffman, A.J.; Cory, M.; McPhail, A.T.; Mailman, R.B. Conformational analysis and molecular modeling of 1-phenyl-, 4-phenyl-, and 1-benzyl-1,2,3,4-tetrahydroisoquinolines as D1 dopamine receptor ligands. *J. Med. Chem.* **1989**, *32*, 2050–2058. [[CrossRef](#)] [[PubMed](#)]
137. Pettersson, F.; Ponten, H.; Waters, N.; Waters, S.; Sonesson, C. Synthesis and evaluation of a set of 4-phenylpiperidines and 4-phenylpiperazines as D2 receptor ligands and the discovery of the dopaminergic stabilizer 4-[3-(methylsulfonyl)phenyl]-1-propylpiperidine (huntsil, pridopidine, ACR16). *J. Med. Chem.* **2010**, *53*, 2510–2520. [[CrossRef](#)]
138. Zheng, Z.; Huang, X.P.; Mangano, T.J.; Zou, R.; Chen, X.; Zaidi, S.A.; Roth, B.L.; Stevens, R.C.; Katritch, V. Structure-Based Discovery of New Antagonist and Biased Agonist Chemotypes for the Kappa Opioid Receptor. *J. Med. Chem.* **2017**, *60*, 3070–3081. [[CrossRef](#)]
139. Nievergelt, A.; Huonker, P.; Schoop, R.; Altmann, K.H.; Gertsch, J. Identification of serotonin 5-HT1A receptor partial agonists in ginger. *Bioorg. Med. Chem.* **2010**, *18*, 3345–3351. [[CrossRef](#)]
140. Maramai, S.; Gemma, S.; Brogi, S.; Campiani, G.; Butini, S.; Stark, H.; Brindisi, M. Dopamine D3 Receptor Antagonists as Potential Therapeutics for the Treatment of Neurological Diseases. *Front. Neurosci.* **2016**, *10*, 451. [[CrossRef](#)]
141. Fan, L.; Tan, L.; Chen, Z.; Qi, J.; Nie, F.; Luo, Z.; Cheng, J.; Wang, S. Haloperidol bound D(2) dopamine receptor structure inspired the discovery of subtype selective ligands. *Nat. Commun.* **2020**, *11*, 1074. [[CrossRef](#)]

**Disclaimer/Publisher's Note:** The statements, opinions and data contained in all publications are solely those of the individual author(s) and contributor(s) and not of MDPI and/or the editor(s). MDPI and/or the editor(s) disclaim responsibility for any injury to people or property resulting from any ideas, methods, instructions or products referred to in the content.